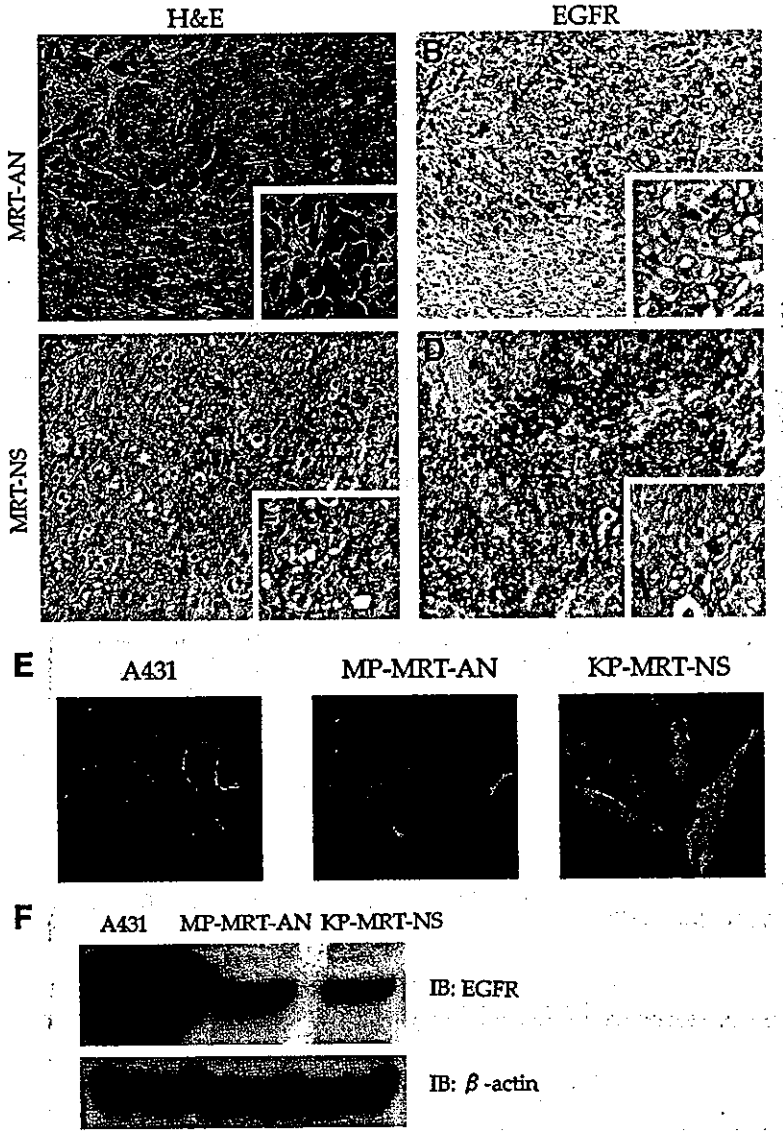

Fig. 2 Expression of EGFR on two MRT clinical tissues and their cell lines. *A–D*, hematoxylin and eosin staining and immunohistochemical staining of EGFR in MRT clinical tissues (*AN* and *NS*; ×200). *Insets*, higher magnifications of the sections in *A–D* (×400). *E*, immunofluorescence staining of two MRT cell lines (*MP-MRT-AN* and *KP-MRT-NS*) with anti-EGFR antibody (×400). The A431 cell line was used as a positive control. *F*, Western blot analysis of EGFR and β-actin expression in the two MRT cell lines. Total cell proteins (35 μg) were separated on a 7.5% SDS-polyacrylamide gel and probed with EGFR antibody. The levels of EGFR protein were quantified as described in Materials and Methods.

Expression of EGFR in two MRT cell lines was quantitatively determined by Western blot. EGFR expression in both MRT cell lines was lower than that in the A431 cell lines. EGFR expression in the MP-MRT-AN cell line was 1.54 ± 0.036 times more than that in the KP-MRT-NS cell line (Fig. 2*F*).

Inhibition of EGFR Phosphorylation by Gefitinib in MRT Cell Lines. Because the two MRT cell lines express surface EGFR, the ability of gefitinib to inhibit EGFR phosphorylation was examined. Baseline phosphorylation of EGFR was absent in both MRT cell lines cultured in serum-free medium (Fig. 3*A*). However, treatment with EGF (50 ng/mL) for 5 minutes induced strong tyrosine phosphorylation of EGFR in both MRT cell lines (Fig. 3*A*). This effect was decreased in a dose-dependent manner by pretreatment with gefitinib (0.01–20 μmol/L) before the addition of EGF (Fig. 3*A*). Inhibition was clearly evident with the concentration of gefitinib as low as 0.01 μmol/L. However, the total amount of EGFR was not changed by EGF, gefitinib, and/or DMSO.

Inhibition of MRT Cell Growth by Gefitinib *In vitro*. Effects of gefitinib on the proliferation of two MRT cell lines were determined *in vitro*. When the two MRT cell lines were treated with gefitinib at concentrations from 0.1 to 100 μmol/L during the linear growth phase, the proliferation of each MRT cell line was inhibited in a dose-dependent manner (Fig. 3, *B* and *C*). In this assay system, the IC_{50} value of the antiproliferation effect of gefitinib was 10 μmol/L in MP-MRT-AN and was 12 μmol/L in

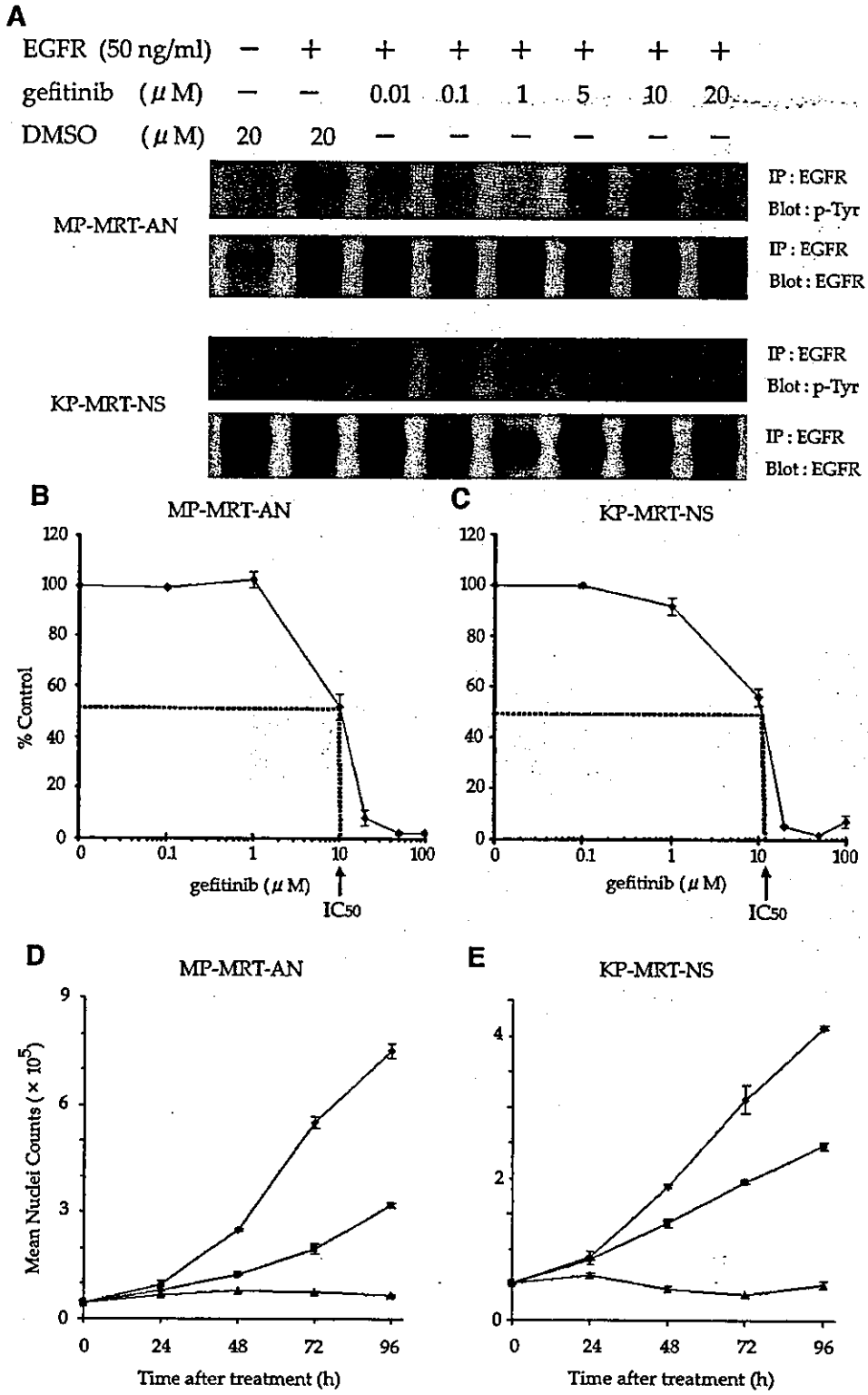

Fig. 3 Effect of gefitinib on two MRT cell lines. *A*, inhibition of EGFR phosphorylation was clearly evident with the concentration of gefitinib as low as 0.01 μmol/L. Cells were placed in serum-free medium for 24 hours and then treated with the indicated concentrations of gefitinib for 30 minutes. Control cells received drug vehicle: DMSO, final concentration 0.2%. Cells were then stimulated (+) or not (−) with EGF for 5 minutes, lysed, and immunoprecipitated with anti-EGFR antibody. Immunoprecipitates were eluted, separated on a 7.5% SDS-polyacrylamide gel, and probed with antiphosphotyrosine antibody (*top*). The blot was then stripped and reprobed with anti-EGFR antibody (*bottom*). Blots are representative of three separate experiments. *IP*, immunoprecipitation; *p-Tyr*, phosphotyrosine. *B* and *C*, inhibition of tumor growth of MRT cell lines by gefitinib. MRT cells were seeded and allowed to attach for 24 hours, and cultured in medium containing serial dilutions of gefitinib for 96 hours in triplicate cultures. Growth was assessed by lysing the cells and counting nuclei. Values are the mean of results from three wells from one of three similar experiments; *bars*, ±SE. IC_{50} values are given in Results. *D* and *E*, cell growth curves of two MRT cell lines. MRT cells were cultured as described above. Cells were harvested every 24 hours, and nuclei were counted. Values are the mean of results from three wells from one of three similar experiments; *bars*, ±SE. ●, Control; ■, gefitinib10 μM; ▲, gefitnib20 μM.

KP-MRT-NS. As shown in Fig. 3, *D* and *E*, the growth of MP-MRT-AN and KP-MRT-NS cells was inhibited after 48 hours of gefitinib treatment (10 or 20 μmol/L).

Next, we attempted to determine whether the inhibition of cell growth by gefitinib was associated with either apoptosis or cytostasis. Tumor cells were harvested every 24 hours after gefitinib treatment (5, 10, or 20 μmol/L), and apoptotic cells were examined by terminal deoxynucleotidyl

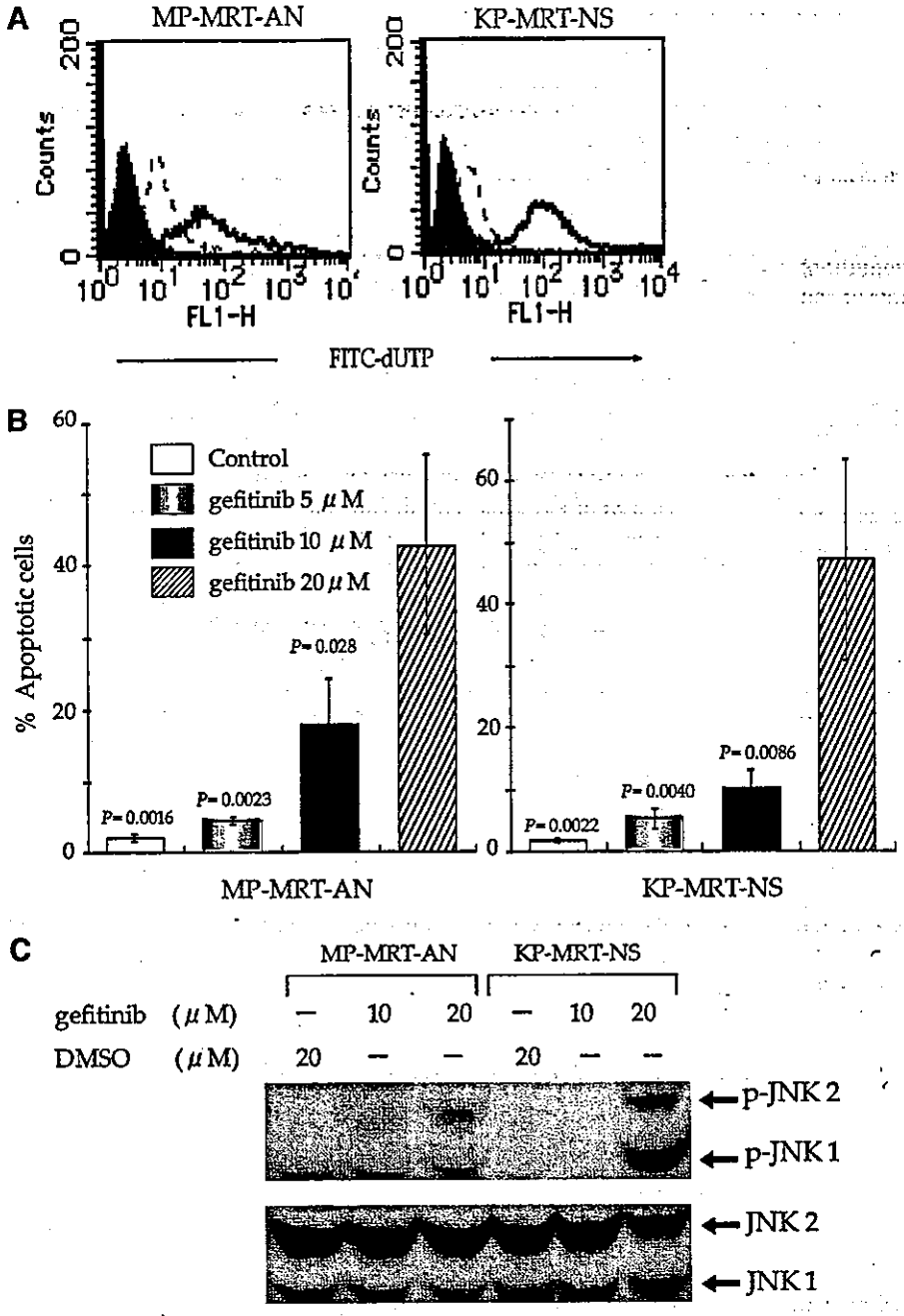

Fig. 4 Induction of apoptosis by gefitinib in two MRT cell lines. *A*, MRT cells were stained with fluorescein isothiocyanate-dUTP after 96 hours of culture with gefitinib and examined by flow cytometry. Histogram shows the induction of apoptotic MRT cells by gefitinib treatment in a dose-dependent manner. The apoptotic cells staining with fluorescein isothiocyanate-dUTP increased after 96 hours of treatment of 20 μmol/L (*solid histograms*) or 10 μmol/L gefitinib (*dashed histograms*) compared with 0.2% DMSO (control; *shaded histograms*). Counts = number of events. *B*, percentages of total apoptotic cells. Percentages were determined as in *A*. Values are the mean of four independent experiences; *bars*, ±SE. *P* values relative to 20 μmol/L gefitinib. *C*, cells were placed in culture medium for 24 hours and then treated with the indicated concentrations of gefitinib for 48 hours. Control cells received drug vehicle: DMSO, final concentration 0.2%. Cells were lysed and separated on a 10% SDS-polyacrylamide gel and probed with anti-pJNK antibody (*top*). The blot was then stripped and reprobed with anti-JNK antibody (*bottom*). Blots are representative of three separate experiments.

transferase-mediated nick end labeling assay (Fig. 4*A*). Apoptosis was observed after 48 hours of gefitinib treatment at concentrations more than the IC_{50} values (data not shown), and the maximum level of apoptosis was observed after 96 hours of gefitinib treatment. The effect of gefitinib on the number of apoptotic cells after 96 hours of treatment was dose dependent. Induction of apoptosis was significantly greater at 20 μmol/L gefitinib (MP-MRT-AN, 42.9% and KP-MRT-NS, 47.2%) than at 5 (MP-MRT-AN, 4.5% and KP-MRT-NS, 5.4%) and 10 μmol/L (MP-MRT-AN, 17.9% and KP-MRT-NS, 10.2%; $P < 0.05$, multiple comparisons using Fisher's projected least significant difference test; Fig. 4*B*). Therefore, growth inhibition of the MP-MRT-AN and KP-MRT-NS cell lines induced by treatment with gefitinib at concentrations equal to or lower than IC_{50} (5 and 10 μmol/L) was due to cytostasis, whereas growth inhibition by gefitinib at a concentration greater than IC_{50} (20 μmol/L) was due to apoptosis.

Phosphorylation of JNK and AKT by Gefitinib in MRT Cell Lines. To determine whether gefitinib treatment induces apoptosis, we examined the effects of gefitinib on the phosphorylation status of signal transduction mediators that are associ-

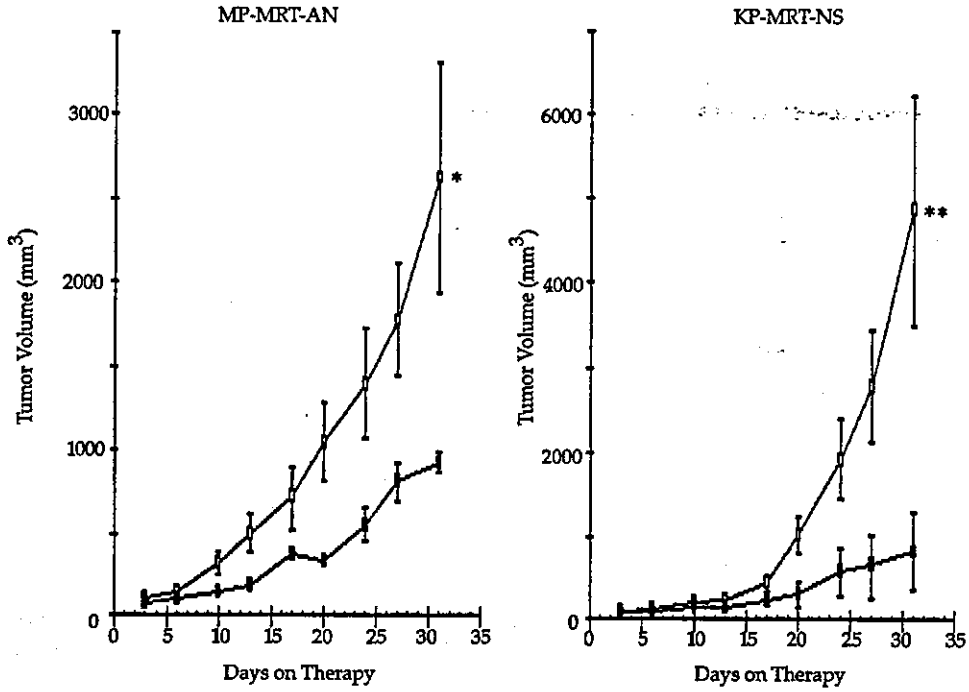

Fig. 5 Inhibition of tumor growth of MRT cell lines (*MP-MRT-AN* and *KP-MRT-NS*) in athymic mice by oral administration of gefitinib. Treatment was started 1 day after tumor injection. Once-daily oral gavages of gefitinib at 150 mg/kg (■), or vehicle alone (□) were given for 27 days (5 days/week). Each group contained 7–8 mice. Values are the mean; *bars*, ±SE. *, $P = 0.039$; **, $P = 0.047$ relative to vehicle alone.

ated with apoptosis or cell survival. Two such mediators, JNK1 and JNK2, have been associated with apoptosis when in their activated (phosphorylated) forms. JNK1 and 2 are isoforms of one another with masses of 46 and 55 kDa, respectively (25–28). AKT is a serine/threonine kinase that promotes cell survival when it is in its active form (29). Gefitinib has been shown to inhibit the phosphorylation of AKT (30). Therefore, we evaluate the phosphorylation of JNK and AKT. When incubated in 20 μmol/L gefitinib for 48 hours, both MRT cell lines expressed phosphorylated JNK 1 and 2 (p-JNK1 and 2). However, when incubated in 10 μmol/L gefitinib, MP-MRT-AN expressed p-JNK-2 but not p-JNK-1, whereas KP-MRT-NS did not express either. Thus, activation of JNK2 was persistent at 48 hours after 20 μmol/L gefitinib treatment in both MRT cell lines (Fig. 4*C*). On the other hand, neither 10 μmol/L nor 20 μmol/L of gefitinib treatment inhibited phosphorylation of AKT in either MRT cell line (data not shown).

Inhibition of Tumor Growth *In vivo*. The antitumor activity of gefitinib *in vivo* was examined by oral administration of gefitinib to athymic mice that had been injected s.c. (*i.e.*, xenografted) with 4×10^6 MRT cells. Gefitinib treatment started 1 day after injection. One week after the injection, 5 of 8 mice xenografted with MP-MRT-AN cells and 8 of 8 mice xenografted with KP-MRT-NS cells had single palpable tumors. Although tumors in vehicle-treated mice grew exponentially, tumors in the gefitinib-treated group grew slowly throughout the course of administration (Fig. 5). Mean tumor volume in the gefitinib-treated group was significantly smaller than that in the vehicle-treated group by day 31, in both the mice xenografted with MP-MRT-AN cells [2633 ± 689 mm^3 ($n = 5$) *versus* 928 ± 65 mm^3 ($n = 5$); $P = 0.039$] and in the mice xenografted with KP-MRT-NS cells [4360 ± 1374 mm^3 ($n = 8$) *versus* 1218 ± 458 mm^3 ($n = 8$); $P = 0.048$]. The experiment was repeated except that gefitinib was started 7 days after tumor injection. Similar results were obtained 24 days after tumor injection, in both the mice xenografted with MP-MRT-AN cells [1116 ± 98 mm^3 ($n = 7$) *versus* 604 ± 76 mm^3 ($n = 7$); $P = 0.0014$] and in the mice xenografted with KP-MRT-NS cells [2841 ± 661 mm^3 ($n = 7$) *versus* 505 ± 150 mm^3 ($n = 6$); $P = 0.0086$ (Fig. not shown)].

Moreover, we evaluated whether apoptotic cells were induced in the tissues of the xenograft. Terminal deoxynucleotidyl transferase-mediated nick end labeling staining was not significantly different between the vehicle-treated group and the gefitinib-treated group (data no shown). This demonstrated that oral administration of gefitinib inhibited tumor growth in athymic mice due to cytostasis.

DISCUSSION

The objective of this study was to determine the effects of gefitinib, an EGFR-tyrosine kinase inhibitor, on MRT cells and to evaluate the potential of gefitinib as a novel agent for treatment of MRT patients. Our results indicate that targeted inhibition of EGFR-tyrosine kinase is a promising therapeutic strategy for MRT patients that are refractory to other treatments.

This is the first report of the expression of EGFR in two clinical MRT tissues by immunohistochemical examination (Fig. 2, *A–D*). Expression of EGFR was also demonstrated in two MRT cell lines derived from these two MRT tissues by immunofluorescence (Fig. 2*E*) and Western blot (Fig. 2*F*). These cell lines have an altered *INI-1* gene (Fig. 1). Alterations in this gene are restricted to MRT in pediatric tumors (12). Our obtained results are consistent with the recent detection of

EGFR expression in five MRT cell lines. Moreover, EGFR was found to be phosphorylated by EGF in two MRT cell lines (Fig. 3*A*). These results prompted us to evaluate the possibility of targeting EGFR for treatment of MRT.

Next, the antitumor effects of gefitinib on two MRT cell lines were evaluated *in vitro*. Treatment of gefitinib induced a dose-dependent growth inhibition *in vitro* in two MRT cell lines (Fig. 3, *B–E*). The growth inhibition induced by gefitinib was due to cytostasis at concentrations near the IC_{50} values, although it was more due to apoptosis at higher doses (Fig. 3, *D* and *E*; Fig. 4*A*). Our IC_{50} values of the inhibition of EGFR phosphorylation (Fig. 3*A*) in MRT cell lines are similar to the IC_{50} value of other cancer cell lines (0.027–0.033 μmol/L; ref. 7). On the other hand, the gefitinib IC_{50} values of growth inhibition of head and neck cancer, lung cancer, and breast cancer cell lines were very close to our results under similar experimental conditions (31, 32). Thus, our results are congruent with those reported by other investigators.

We showed that 20 μmol/L gefitinib treatment resulted in persistent phosphorylation of JNK2 (Fig. 4*C*). JNK activation is induced by sources of stress such as UV light, cytokines, and cytotoxic drugs via mitogen-activated protein kinase kinases 7 and 4 (25). On the other hand, Singh *et al.* (28) have reported that dephosphorylation of EGFR leads to an increase in phosphorylated JNK1 and 2, and other investigators have reported that persistent activation of JNK1 (26) or activation of JNK2 (29) induce apoptosis. Thus, our results suggests that apoptosis by gefitinib is associated with the JNK pathway via EGFR in MRT cell lines. Moreover, inhibition of AKT activity correlates well with sensitivity to gefitinib (31). However, the importance of AKT inhibition by gefitinib may differ among different tumor types (31). On the basis of our results with MRT cell lines, apoptosis induced by gefitinib is associated with the JNK pathway.

We found that 150 mg/kg gefitinib treatment had no significant apoptotic change in MRT xenograft tissues. The maximum nonlethal dose of gefitinib in mice was reported to be 150 mg/kg (8). Because this is the same concentration at which gefitinib had a cytostatic effect against established MRT xenografts (Fig. 5), the *in vivo* effect of gefitinib in MRT cells might be limited to the cytostatic effect. Christensen *et al.* (10) showed that the plasma concentrations of mice given gefitinib orally at a dose of 100 mg/kg for 2 days reached 7 μmol/L. In the present study, the plasma gefitinib concentrations of mice given gefitinib at 150 mg/kg might reach to the levels of 10 μmol/L. Therefore, in accordance with the *in vitro* results, gefitinib did not induce apoptosis *in vivo*.

Human tumor xenograft studies have indicated that gefitinib can inhibit the growth of tumors having many EGFR levels (7, 8, 9, 10). In these studies, as in the present study, the effect of gefitinib at the dose of 100–150 mg/kg was cytostasis. Because the inhibition of tumor cell growth by gefitinib in our study was observed *in vitro* as well as *in vivo*, our results provide a rationale for evaluating the anticancer activity of gefitinib in patients with MRT.

In a Phase I study, the maximal plasma concentration of gefitinib at the dose of 700 mg/day varied over a wide range (3–7 μmol/L; ref. 33). Gefitinib is metabolized in the liver via the cytochrome P450 3A4 (CYP3A4) pathway (34). The pharmacokinetics of gefitinib in children is not well known. However, because CYP3A4 activity of infants is lower than that of adults (35), it may be possible to achieve plasma gefitinib concentrations of 10 μmol/L and to demonstrate antitumor effects in infant MRT patients.

Oral gefitinib was found to have meaningful antitumor activity in a randomized Phase II trial (13). The response of non-small-cell lung cancers to gefitinib in the above clinical trial was related to adenocarcinoma histology, although high EGFR expression is more common in squamous carcinomas than in adenocarcinomas (11). Thus, the clinical response to gefitinib is not related to the amount of EGFR expression, and the target of gefitinib has not been well clarified.

Indeed, induction of apoptosis and inhibition of growth of MRT cell lines by gefitinib required higher concentrations of gefitinib (20 μmol/L and IC_{50} = 10–12 μmol/L, respectively) than the inhibition of EGFR phosphorylation (IC_{50} < 0.1 μmol/L) in a cell-based assay. One possible explanation for the discrepancy in IC_{50} values between the inhibition of EGFR phosphorylation and cell growth is that the action of gefitinib in MRT may involve inhibition of other tyrosine kinases. Our immunofluorescence studies demonstrated that EGFR expression among the same MRT cells is heterogeneous (Fig. 2*E*), and EGFR expression levels between the two MRT cell lines are different (Fig. 2*F*). Thus, the uniformity of gefitinib sensitivity in MRT cell lines raises the possibility that some other tyrosine kinases are involved in gefitinib. The verification of targets of gefitinib and the functions of EGFR in MRT cells may be relevant to the understanding of the molecular basis and pathogenesis of MRT.

MRT is notoriously refractory to present anticancer drugs. Our results indicate that gefitinib may make a positive contribution to the therapy of MRT patients. Additional studies are needed to determine what functions EGFR has in MRT cells and whether MRT patients expressing EGFR tend to have poor prognoses. Moreover, additional clinical trials of MRT patients are needed to determine the efficacy and targets of gefitinib. Because the number of MRT patients is small, such trials may need to be global.

In conclusion, our results demonstrated that gefitinib has antitumor effects on MRT *in vitro* and *in vivo* and could be a novel therapeutic agent for improving the prognosis of MRT.

ACKNOWLEDGMENTS

We are grateful to Dr. Keiichi Yokoyama for helpful advice about the histopathology of MRT tissues and to Dr. Shinji Akioka for useful advice about RT-PCR.

REFERENCES

1. Beckwith JB, Palmer NF. Histopathology and prognosis of Wilms' tumor.: Results from the first national Wilms' tumor study. Cancer 1978;41:1937–48.

2. D'Angio GJ, Breslow N, Beckwith JB, et al. Treatment of Wilms' Tumor. : Results of the third national Wilms' tumor study. Cancer 1989 Jul 15;64:349–60.

3. Palmer DM, Weeks DA, Beckwith JB. The clinicopathologic Spectrum of putative extrarenal rhabdoid tumors. An analysis of 42 cases studied with immunohistochemistry or electron microscopy. Am J Sur Pathol 1994;18:1010–29.

4. Tomlinson GE, Breslow NE, Moksness J, Beckwith JB, D'Angio GJ, Green DM. Prognostic factors in rhabdoid tumor of the kidney: Results of the national Wilms' tumor study group (NWTSG). Proc Am Soc Clin Oncol 1996;15:460.

5. Nicholson RI, Gee JMW, Harper ME. EGFR and cancer prognosis. Eur J Cancer 2001;37:S9–15.

6. Holbro T, Civenni G, Hynes NE. The ErbB receptors and their role in cancer progression. Exp Cell Res 2003;284:99–110.

7. Wakeling AE, Guy SP, Woodburn JR, et al. ZD1839 (Iressa): An orally active inhibitor of epidermal growth factor signaling with potential for cancer therapy. Cancer Res 2002;62:5749–54.

8. Sirotnak FM, Zakowski MF, Miller VA, Scher HI, Kris MG. Efficacy of cytotoxic agents against human tumor xenografts is markedly enhanced by coadministration of ZD1839 (Iressa), an inhibitor of EGFR tyrosine kinase. Clin Cancer Res 2000;6:4885–92.

9. Ciardiello F, Caputo R, Bianco R, et al. Antitumor effect and potentiation of cytotoxic drugs activity in human cancer cells by ZD1839 (Iressa), an epidermal growth factor receptor-selective tyrosine kinase inhibitor. Clin Cancer Res 2000;6:2053–63.

10. Christensen JG, Schreck RE, Chan E, et al. High levels of HER-2 expression alter the ability of epidermal growth factor receptor (EGFR) family tyrosine kinase inhibitors to inhibit EGFR phosphorylation in vivo. Clin Cancer Res 2001;7:4230–8.

11. Fukuoka M, Yano S, Giaccone G, et al. Multi-institutional randomized phase II trial of gefitinib for previously treated patients with advanced non-small-cell lung tumor. J Clin Oncol 2003;21:2237–46.

12. Uno K, Takita J, Yokomori K, et al. Aberrations of the hSNF/INI1 gene are restricted to malignant rhabdoid tumors or atypical teratoid/rhabdoid tumors in pediatric solid tumors. Gene Chromosome Cancer 2002;34:33–41.

13. Sugimoto T, Hosoi H, Horii Y, et al. Malignant rhabdoid-tumor cell line showing neural and smooth-muscle-cell phenotypes. Int J Cancer 1999;82:678–86.

14. Narita T, Taga T, Sugita K, Nakazawa S, Ohta S. The autocrine loop of epidermal growth factor receptor-epidermal growth factor/transforming growth factor-α in malignant rhabdoid tumor cell lines: heterogeneity of autocrine mechanism in TTC549. Jpn J Cancer Res 2001; 92:269–78.

15. Mori T, Fukuda Y, Kuroda H, et al. Cloning and characterization of a novel Rab-family gene, Rab36, within the region at 22q11.2 that is homozygously deleted in malignant rhabdoid tumors. Biochem Biophys Res Commun 1999;254:594–600.

16. Versteege I, Sevenet N, Lange J, et al. Truncating mutations of hSNF5/INI1 in aggressive paediatric cancer. Nature 1998 Jul 9;394: 203–7.

17. Waterfield MD, Mayes ELV, Stroobant P, et al. A monoclonal antibody to the human epidermal growth factor receptor. J Cell Biochem 1982;20:149–61.

18. Ishida H, Matsumura T, Salgaller ML, Ohmizono Y, Kadono Y, Sawada T. MAGE-1 and MAGE-3 OR-6 expression in neuroblastoma-related pediatric solid tumors. Int J Cancer 1996;69:375–80.

19. Biegel JA, Zhou JY, Rorke LB, Stenstrom C, Wainwright LM, Fogelgren B. Germ-line and acquired mutations of INI1 in atypical teratoid and rhabdoid tumors. Cancer Res 1999;159:74–9.

20. Vyberg M, Nielsen S. Dextran polymer conjugate Two-step Visualization system for immunohistochemistry: a comparison of EnVision+ with two three-step avidin-biotin techniques. Appl Immunohistochemistry 1998;6:3–10.

21. Butler WB. Preparing nuclei from cells in monolayer cultures suitable for counting and for following synchronized cells through the cell cycle. Anal Biochem 1984;141:70–3.

22. Dilling MB, Dias P, Shapiro DN, Germain GS, Johnson RK, Houghton PJ. Rapamycin selectively inhibits the growth of childhood rhabdomyosarcoma cells through inhibition of signaling via the type I Insulin-like growth factor receptor. Cancer Res 1994;54:903–7.

23. Misawa A, Hosoi H, Arimoto A, et al. N-Myc induction stimulated by insulin-like growth factor I through mitogen-activated protein kinase signaling pathway in human neuroblastoma cells. Cancer Res 2000 Jan 1;60:64–9.

24. Gavrieli Y, Sherman Y, Ben-Sasson SA. Identification of programmed cell death in situ via specific labeling of nuclear DNA fragmentation. J Cell Biol 1992;119:493–501.

25. Davis RJ. Signal transduction by the JNK group of MAP kinases. Cell 2000;10:239–52.

26. Chen YR, Meyer CF, Tan TH. Persistent activation of c-Jun N-terminal kinase 1 (JNK1) in γ radiation-induced apoptosis. J Biol Chem 1996;271:631–4.

27. Bhrens A, Sabapathy K, Graef I, Cleary M, Crabtree GR, Wagner EF. Jun N-terminal kinase 2 modulates thymocyte apoptosis and T cell activation through c-Jun and nuclear factor of activated T cell (NF-AT). Proc Natl Acad Sci 1998;98:1769–74.

28. Singh F, Gao D, Lebwohl MG, Wei H. Shikonin modulates cell proliferation by inhibiting epidermal growth factor receptor signaling in human epidermoid carcinoma cells. Cancer Lett 2003;200:115–21.

29. Kennedy SG, Kandel ES, Cross TK, Hay N. Akt/protein kinase B inhibits cell death by preventing the release of cytochrome c from mitochondria. Mol Cell Biol 1999;19:5800–10.

30. Jänne PA, Taffaro ML, Salgia R, Johnson BE. Inhibition of epidermal growth factor receptor signaling in malignant pleural mesothelioma. Cancer Res 2002 Sep 15;62:5242–7.

31. Moasser MM, Basso A, Averbuch SD, Rosen N. The tyrosine kinase inhibitor ZD1839 ("Iressa") inhibits HER-2-driven signaling and suppresses the growth of HER-2overexpressing tumor cells. Cancer Res 2001;61:7184–8.

32. Magne N, Fischel JL, Dubreuil A, et al. Influence of epidermal growth factor (EGFR), p53 and intrinsic MAP kinase pathway status of tumour cells on the antiproliferative effect of ZD1839. Br J Cancer 2002;86:1518–23.

33. Ranson M, Hammond LA, Ferry D, et al. ZD1839, a selective oral epidermal growth factor receptor-tyrosine kinase inhibitor is well tolerated and active in patients with solid, malignant tumors: results of a phase I trial. J Clin Oncol 2002;20:2240–50.

34. Culy CR, Faulds D. Gefitinib. Drugs 2002;62:2237–48.

35. Johnson TN, Tanner MS, Taylor CJ, Tucker GT. Enterocytic CYP3A4 in a pediatric population: developmental changes and the effect of celiac disease and cystic fibrosis. Br J Clin Pharmacol 2001; 51:451–60.

Int. J. Cancer: 112, 219–224 (2004)

Publication of the International Union Against Cancer

FENRETINIDE INDUCES SUSTAINED-ACTIVATION OF JNK/p38 MAPK AND APOPTOSIS IN A REACTIVE OXYGEN SPECIES-DEPENDENT MANNER IN NEUROBLASTOMA CELLS

Shinya OSONE*, Hajime HOSOI, Yasumichi KUWAHARA, Yoshifumi MATSUMOTO, Tomoko IEHARA and Tohru SUGIMOTO

Department of Pediatrics, Kyoto Prefectural University of Medicine, Graduate School of Medical Science, Kyoto, Japan

Fenretinide, which mediates apoptosis in neuroblastoma cells, is being considered as a novel therapeutic for neuroblastoma. The cytotoxic mechanisms of fenretinide, however, have not been fully elucidated. Sustained-activation of JNK and p38 MAPK signaling has been shown recently to have a pivotal role in stress-induced apoptosis. Whether fenretinide activates the signaling in neuroblastoma cells is not known. In the present study, fenretinide induced sustained-activation of both JNK and p38 MAPK in neuroblastoma cells. Pretreatment with the antioxidant L-ascorbic acid almost completely inhibited the accumulation of fenretinide-induced intracellular reactive oxygen species (ROS), activation of JNK and p38 MAPK and apoptosis. Intracellular ROS production and activation of stress signaling was not altered by fenretinide in resistant neuroblastoma cells. Our study demonstrates that in neuroblastoma cells, fenretinide induces sustained-activation of JNK and p38 MAPK in an ROS-dependent manner and indicates that JNK and p38 MAPK signaling might mediate fenretinide-induced apoptosis. Our results also indicate that suppression of the fenretinide-induced ROS productive system and the downstream JNK and p38 MAPK signaling pathways causes neuroblastoma cells to become resistant to fenretinide.

Key words: *fenretinide; neuroblastoma; apoptosis; reactive oxygen species; JNK; p38 MAPK*

Neuroblastoma (NB) is one of the common malignant solid tumors in childhood, arising from neural crest progenitors. Despite progress with multimodal therapies consisting of multidrug chemotherapy, surgical and radiation therapy, the prognosis of advanced NB remains poor.[1] Therefore, new therapeutic approaches are needed. Retinoic acids (RA), which are vitamin A analogs, have been shown to induce the differentiation of NB cells into mature neuronal cells.[2] It has been reported recently that oral administration of 13-cis RA after consolidated chemotherapy with stem cell transplantation improved the 3-year event-free survival of advanced NB patients.[3] Retinoic acids are expected to be used as new therapeutic agents against NB, in view of their relatively low toxicity.

N-(4-hydroxyphenyl) retinamide, also called fenretinide (FR), has cytotoxic activity against various tumor cells including NB.[4] An advantage of FR is that its systemic toxicity is less than that of RA.[5,6] The cytotoxicity of FR is due mainly to its ability to induce apoptosis, although the mechanism has not been fully elucidated.[4] Several studies have shown that, in NB cell lines, FR produced intracellular reactive oxygen species (ROS).[7–9] In addition, FR increases intracellular ceramide, which is known as an inducer of apoptosis, in NB cells.[7,10,11]

Mitogen-activated protein kinases (MAPK) are well-conserved signaling proteins in eukaryotic cells and have essential roles in deciding cell fate.[12,13] Two members of the MAPK family, c-Jun N-terminal kinase (JNK) and p38 MAPK, are activated by various stress stimuli including oxidative stress and chemical agents.[12–14] When activated, they phosphorylate downstream transcription factors of c-Jun and activating transcription factor-2 (ATF-2). Sustained-activation of JNK and p38 MAPK induces cell death.[13,15]

In prostate carcinoma cell lines, FR did not activate p38 MAPK, but it did activate JNK in an ROS-independent manner,[16] and the JNK pathway mediated FR-induced apoptotic signaling.[16,17] It has also been shown that FR activated JNK in A431 epidermoid carcinoma cells.[18] It is not known, however, whether FR activates JNK and p38 MAPK signaling in NB cells, or whether signaling is essential for FR-induced apoptosis. We examined stress signaling and apoptosis induced by FR in NB cells. We found that FR induced sustained-activation of both JNK and p38 MAPK in NB cells, indicating that JNK and p38 MAPK mediate FR-induced apoptosis. We also examined the relationship between the FR-induced ROS generation and the JNK/p38 MAPK signaling, and found that their activation is ROS-dependent. Moreover, we demonstrated that FR failed to produce intracellular ROS and to activate the kinases in the resistant NB cells, indicating the suppression of FR-induced ROS production and activation of JNK/p38 MAPK is one of the mechanisms of resistance to FR in NB cells.

MATERIAL AND METHODS

Cell culture

Human NB cell lines KP-N-TK[19] and KP-N-SIFA[20] were cultured in RPMI 1640 containing penicillin (100 U/ml), streptomycin (100 μg/ml) and 10% heat-inactivated FBS at 37°C in a 5% CO_2 incubator. The medium was changed every 3–4 days. Cells were sub-cultured into new flasks by trypsinization when in a sub-confluent state. FR-resistant cells of KP-N-TK, designated as KP-N-TK (FR-R), were established by culturing parental KP-N-TK cells with increasing concentrations of FR from 0.5–5 μM for 150 days. The cells were then maintained continuously in 5 μM FR.

Antibodies and reagents

Polyclonal antibodies against JNK, p38 MAPK, Thr^{183}/Tyr^{185}-phosphorylated JNK, Thr^{180}/Tyr^{182}-phosphorylated p38 MAPK were purchased from Cell Signaling Technology (Beverly, MA). Monoclonal anti-caspase-3 antibody was from BD Biosciences (San Jose, CA). Monoclonal anti-caspase-9 and anti-poly (ADP-ribose) polymerase (PARP) antibodies were obtained from Oncogene Research Products (San Diego, CA). FR (Toronto Research

Abbreviations: AA, L-ascorbic acid; CM-H_2DCFDA, 5(-6)-chloromethyl-2′-7′-dichlorodihydrofluorescein diacetate; FR, fenretinide; JNK, c-Jun N-terminal kinase; NB, neuroblastoma; p38 MAPK, p38 mitogen-activated protein kinase; PARP, poly (ADP-ribose) polymerase; ROS, reactive oxygen species; TUNEL, TdT-mediated dUTP-biotin nick end labeling.

Grant sponsor: Ministry of Education, Culture, Sports, Science and Technology, Japan; Grant number: 14370250, 15659248, 15659249; Grant sponsor: Ministry of Health and Welfare, Japan; Grant number: 13-19.

*Correspondence to: Department of Pediatrics, Kyoto Prefectural University of Medicine, Graduate School of Medical Science. 465 Kajii-cho, Kamigyo-ku, Kyoto 602-8566, Japan. Fax: +81-75-252-1399.
E-mail: shinn-o@koto.kpu-m.ac.jp

Received 30 September 2003; Accepted 6 April 2004

DOI 10.1002/ijc.20412
Published online 10 June 2004 in Wiley InterScience (www.interscience.wiley.com).

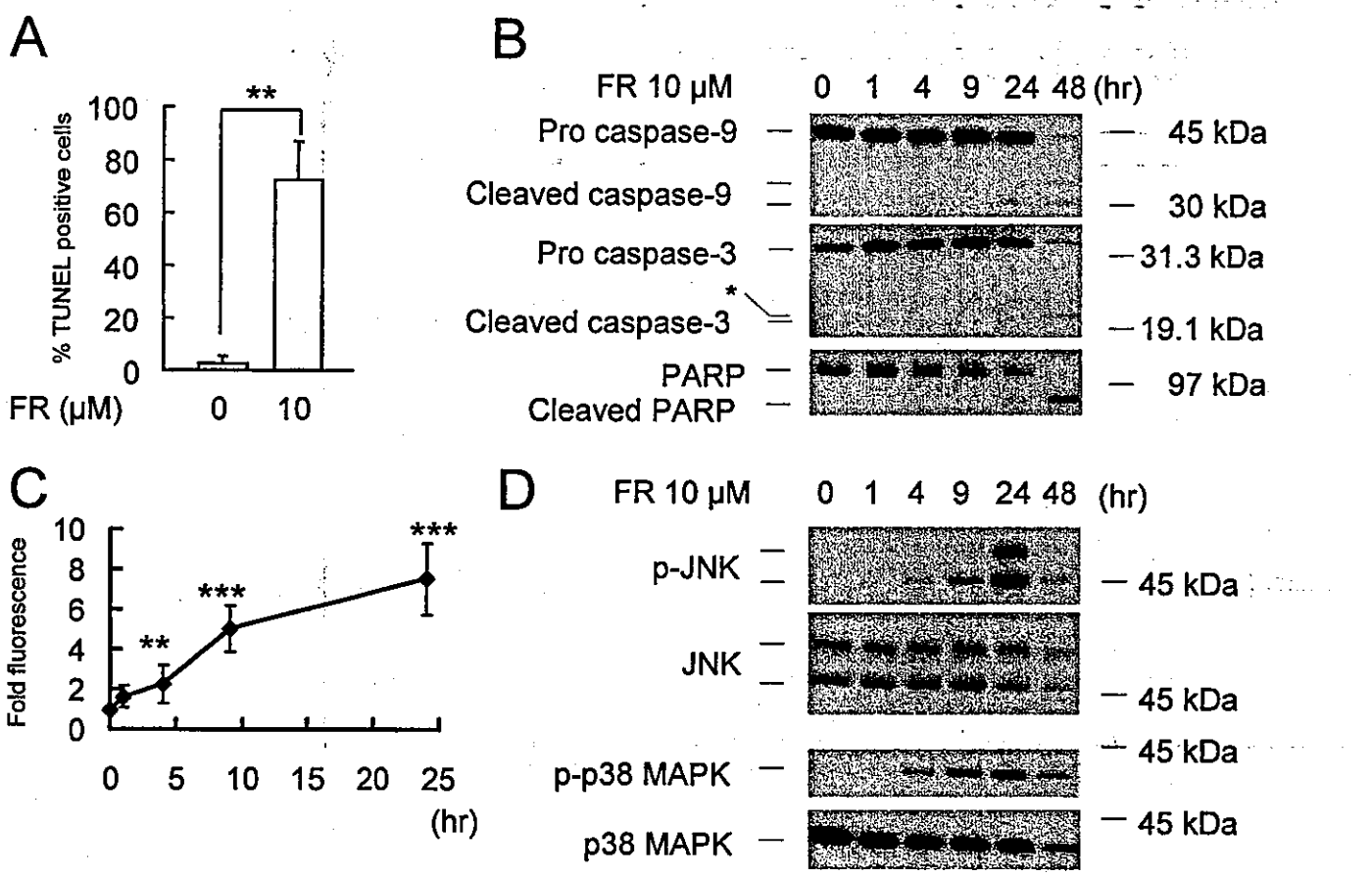

FIGURE 1 – Fenretinide-induced apoptosis, intracellular ROS accumulation and activation of JNK and p38 MAPK in KP-N-TK cells. (*a*) TUNEL assay. Cells were incubated with 10 μM FR or DMSO vehicle for 48 hr. Harvested cells were fixed as described in Material and Methods. After the TdT reaction with FITC labeling, cells were analyzed with a flow cytometer, and the percentage of TUNEL-positive cells was determined (mean + SD, $n = 3$). $^{**}p < 0.01$ (Student's *t*-test). (*b*) Time-course of cleavages of caspase-9, caspase-3 and PARP. Cells were treated with 10 μM FR for the times indicated. Lysates were prepared and immunoblotted for anti-caspase-9, anti-caspase-3 or anti-PARP antibodies. This is representative of 3 independent experiments. The band indicated by an asterisk is a non-specific band. (*c*) Time-course of intracellular ROS accumulation. Cells were incubated with 10 μM FR for the times indicated. CM-H_2DCFDA was added for 2 hr before cell harvesting. Flow cytometric analysis was carried out and the mean fluorescence was calculated (mean + SD, $n = 7$). $^{**}p < 0.01$, $^{***}p < 0.001$ (compared to control, Student's *t*-test) (*d*) Time-course of the activation of JNK and p38 MAPK. Cells were incubated with 10 μM FR for the times indicated. Immunoblotting was carried out using anti-phospho (p)-JNK, anti-JNK, anti-p-p38 MAPK or anti-p38 MAPK. This is representative of 3 independent experiments.

Chemicals, North York, Canada) was dissolved in dimethyl sulfoxide (DMSO) and stored at −70°C in the dark. L-Ascorbic acid (AA) (Wako Pure Chemical Ind., Osaka, Japan) was dissolved in distilled water and stored at −20°C. 5(-6)-Chloromethyl-2′-7′-dichlorodihydrofluorescein diacetate (CM-H_2DCFDA) (Molecular Probes, Eugene, OR) was freshly prepared in DMSO before use. The final concentration of DMSO was <0.2% in all experiments.

Western blotting

Cells (5×10^6) were seeded onto 100-mm dishes. When 50–60% confluence was achieved, cells were treated with 10 μM FR at 37°C with or without pretreatment of 400 μM AA for 12 hr. After the indicated periods, cells were washed once with ice-cold PBS. Floating cells were also collected. Cells were solubilized in RIPA buffer (150 mM NaCl, 50 mM Tris pH 8.0, 1% Nonidet P-40, 0.5% deoxycholate, 0.1% sodium dodecyl sulfate). Protein concentration was determined using a DC protein assay (Bio-Rad Laboratories, Hercules, CA). Cell lysates were electrophoresed on SDS-polyacrylamide gels, and then transferred to a PVDF membrane. The membrane was blocked in Tris-buffered saline (TBS) with 0.1% Tween 20 (TBS-T) and 5% nonfat skim milk, and subsequently probed with the primary antibody. The blots were washed in TBS-T and treated with the appropriate secondary antibodies (Amersham, Arlington, IL), and then analyzed using the ECL chemiluminescence system (Amersham).

Apoptosis assay

Apoptosis was determined using the MEBSTAIN Apoptosis Detection Kit Direct (Medical & Biological Laboratories Co., Nagoya, Japan) according to the manufacturer's protocol. In brief, cells (2×10^6) were plated onto 60-mm dishes. At 50–60% confluence, cells were treated with 10 μM FR at 37°C with or without preincubation with 400 μM AA for 12 hr. After 48 hr, cells were harvested, washed with PBS, and then fixed with 4% paraformaldehyde for 30 min at 4°C. Subsequently, cells were permeabilized with 70% ethanol for more than 30 min at −20°C, and incubated with the mixture of TdT and FITC-conjugated dUTP for 1 hr at 37°C. The cells were analyzed with a FACS Calibur flow cytometer (Nippon Becton Dickinson Co., Tokyo, Japan) and the number of the TUNEL (TdT-mediated dUTP-biotin nick end labeling)-positive cells was calculated using Cell Quest software (Nippon Becton Dickinson Co.).

The cleavages of caspase-9, caspase-3 and PARP were also detected by Western blotting as described above.

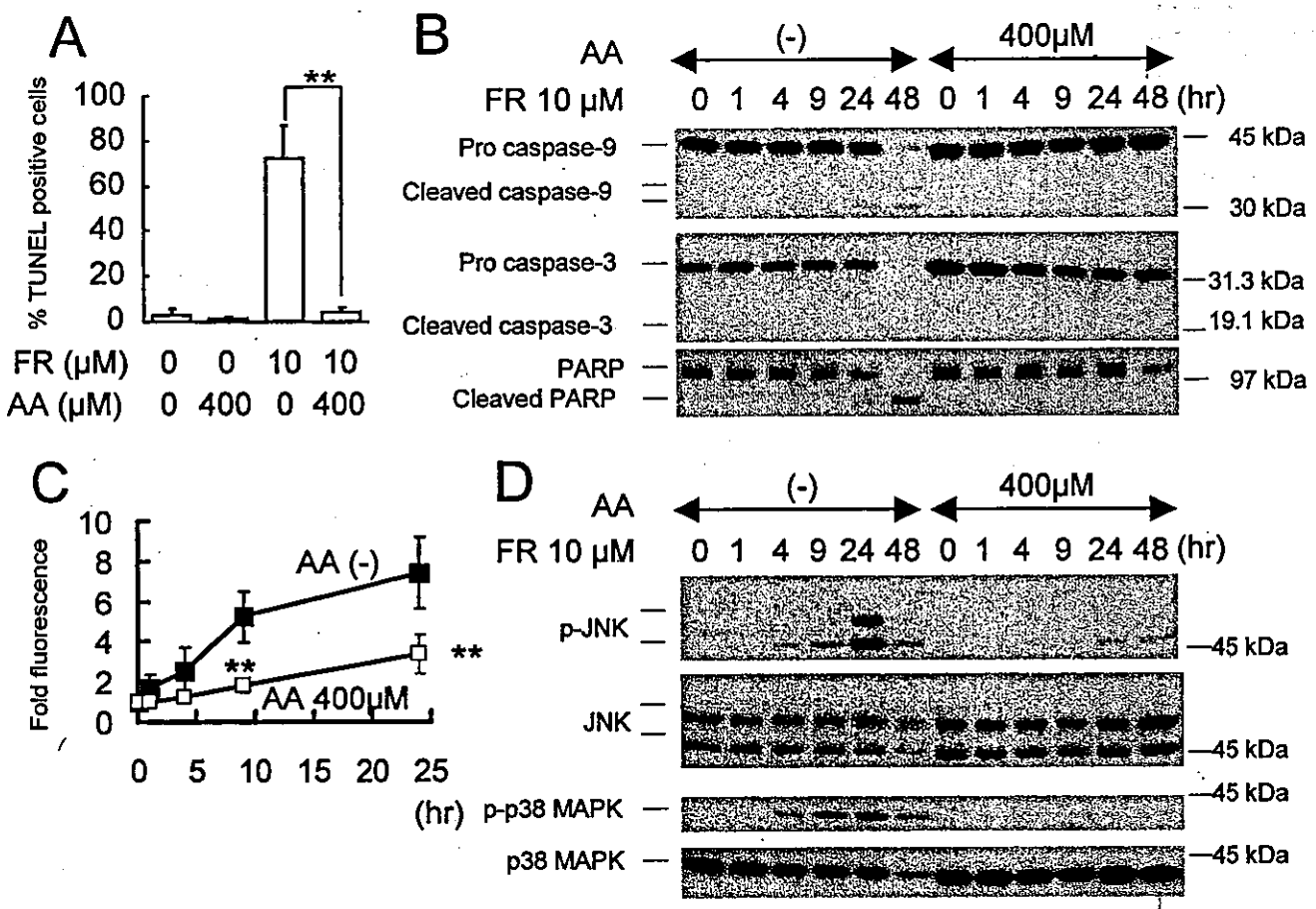

FIGURE 2 – L-Ascorbic acid (AA) inhibits FR-induced apoptosis, ROS accumulation and activation of JNK and p38 MAPK in KP-N-TK cells. Cells were treated with 10 μM FR with or without pretreatment with 400 μM AA for 12 hr. (*a*) TUNEL assay. Cells were incubated with FR or DMSO vehicle for 48 hr. TUNEL assay was carried out as described in Figure 1 (mean + SD, $n = 3$). $^{**}p < 0.01$ (Student's *t*-test). (*b*) Time-course of cleavages of caspase-9, caspase-3 and PARP. Cells were incubated with FR for the times indicated. Immunoblot analysis was carried out as described in Figure 1. This is representative of 3 independent experiments. (*c*) Time-course of intracellular ROS accumulation. Flow cytometric analysis using CM-H_2DCFDA was carried out as described in Figure 1 (mean + SD, $n = 4$). $^{**}p < 0.01$ (Student's *t*-test, compared to no pretreatment of AA). (*d*) Time-course of activation of JNK and p38 MAPK. Cells were incubated with FR for the times indicated with or without pretreatment with AA. Western blot analysis was carried out as described in Figure 1. This is representative of 3 independent experiments.

Determination of intracellular ROS

The intracellular concentration of ROS was measured using CM-H_2DCFDA as a probe. This probe is a non-polar compound that readily diffuses into cells, where it is hydrolyzed to the non-fluorescent polar derivative 2',7'-dichlorofluorescin and thereby trapped within the cells. In the presence of a proper oxidant, 2',7'-dichlorofluorescin is oxidized to highly fluorescent 2',7'-dichlorofluorescein. Cells were plated onto 6-well dishes (5×10^5 cells /well) and treated with 10 μM FR with or without pretreatment of 400 μM AA as above. Two hours before cell harvest, 5 μM CM-H_2DCFDA was added to the cells. After the indicated periods, the medium was removed; cells were washed once with PBS, harvested, and suspended in PBS. The cells were immediately analyzed with a FACS Calibur flow cytometer; the excitation and emission wavelengths were at 488 nm and 530 nm, respectively. The mean fluorescence of 1×10^4 cells per sample was calculated using Cell Quest software.

RESULTS

Fenretinide induces apoptosis, intracellular ROS production and sustained-activation of JNK and p38 MAPK in KP-N-TK NB cells

We first studied FR-induced apoptosis in KP-N-TK cells. After 48 hr incubation with 10 μM FR, up to 70% of the cells were TUNEL-positive (Fig. 1*a*). The DMSO vehicle did not induce apoptosis (Fig. 1*a*). Cleavages of caspase-9, caspase-3 and PARP appeared 24 hr after the treatment, and progressed at 48 hr (Fig. 1*b*). We then studied the intracellular ROS production by FR in KP-N-TK cells. The fluorescence of CM-H_2DCFDA increased gradually during 24 hr of incubation with 10 μM FR (Fig. 1*c*). DMSO vehicle alone did not increase the fluorescence (data not shown).

Fenretinide induced sustained-activation of both JNK and p38 MAPK in KP-N-TK cells (Fig. 1*d*). The phosphorylation of JNK and p38 MAPK was observed from 4–48 hr after treatment with 10 μM FR, and peaked at 24 hr after treatment. The total amounts of JNK and p38 MAPK decreased at 48 hr. Short incubation with FR from 15 min (data not shown) and 1 hr (Fig. 1*d*) did not activate these kinases. The DMSO vehicle alone also did not alter their activation (data not shown).

L-Ascorbic acid suppresses fenretinide-induced apoptosis, intracellular ROS accumulation and activation of JNK and p38 MAPK

KP-N-TK cells were pretreated with 400 μM of the antioxidant AA and then incubated with 10 μM FR for 48 hr. Pretreatment with AA almost completely blocked FR-induced apoptosis (Fig. 2*a*). Fenretinide-induced processing of caspase-9, caspase-3 and PARP was also suppressed in the presence of AA (Fig. 2*b*).

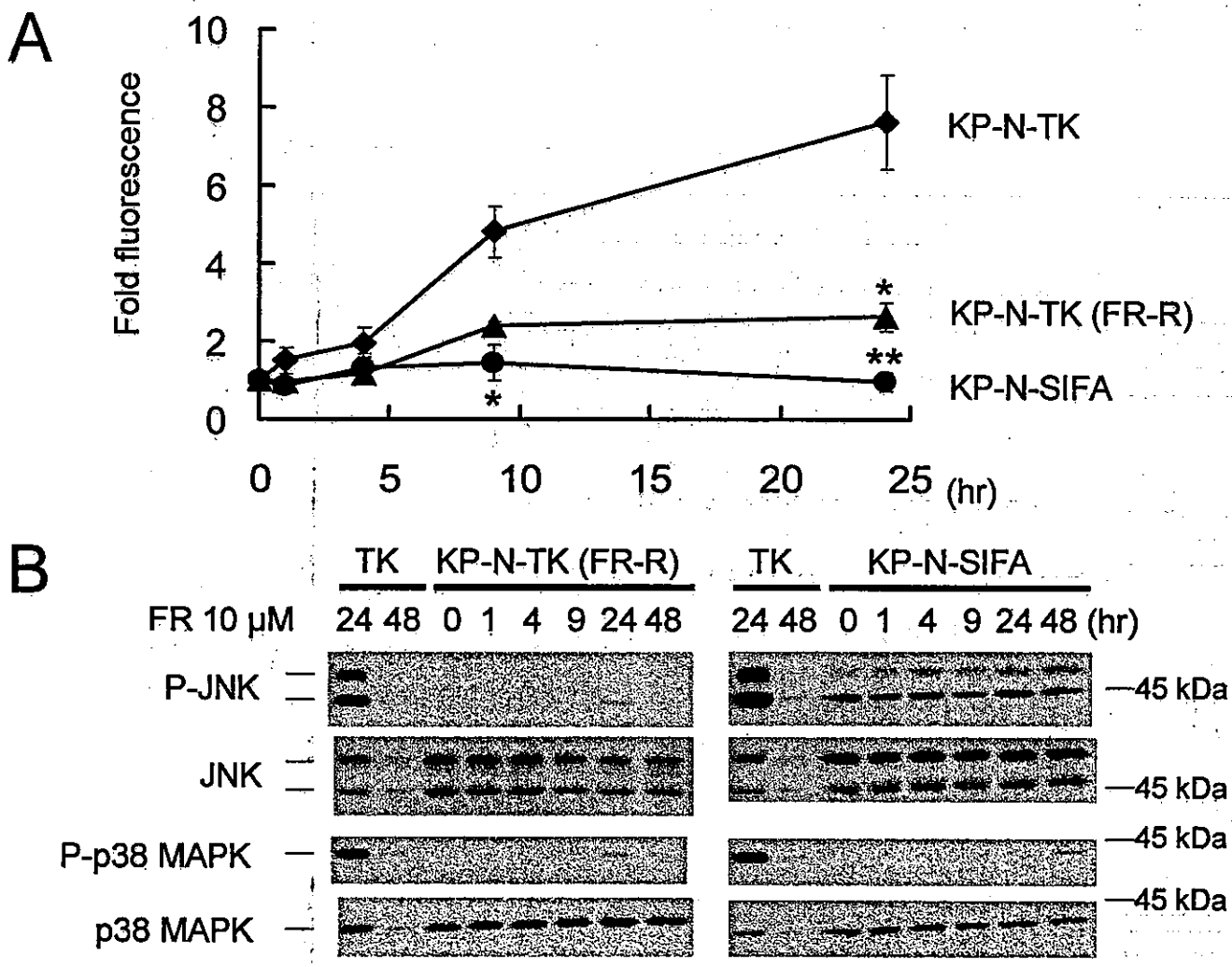

FIGURE 3 – Fenretinide-induced ROS accumulation and activation of JNK and p38 MAPK is suppressed in FR-resistant KP-N-TK (FR-R) and KP-N-SIFA cells. (*a*) Time-course of intracellular ROS. Cells were incubated with 10 μM FR for the times indicated. CM-H_2DCFDA was added for 2 hr before cell harvesting. Flow cytometric analysis was carried out and the mean fluorescence was calculated (mean ± SD, $n = 3$). $^*p < 0.05$, $^{**}p < 0.01$ (compared to KP-N-TK, Student's *t*-test). (*b*) Time-course of activation of JNK and p38 MAPK. Cells were treated with 10 μM FR for the times indicated. Immunoblotting was carried out as described above. This is representative of 3 independent experiments.

Furthermore, preincubation of AA suppressed FR-induced intracellular ROS accumulation in KP-N-TK cells (Fig. 2*c*). To determine whether FR-induced activation of JNK and p38 MAPK is ROS-dependent, we compared the phosphorylation of JNK and p38 MAPK induced by FR with or without preincubation with AA in KP-N-TK cells. In the presence of AA, FR-induced activation of JNK and p38 MAPK was suppressed markedly (Fig. 2*d*).

Fenretinide-induced intracellular ROS accumulation and activation of JNK and p38 MAPK is decreased in fenretinide-resistant NB cell lines

To investigate the mechanism of resistance to FR in NB cells, we generated a FR-resistant KP-N-TK cell line, KP-N-TK (FR-R) cells. KP-N-TK (FR-R) was highly resistant to FR even at a concentration of 10 μM FR (data not shown). When KP-N-TK (FR-R) was incubated in FR-free medium, its resistance to FR was preserved (data not shown). KP-N-SIFA cells exhibited complete resistance to 10 μM FR (data not shown).

To determine whether FR-induced intracellular ROS production was altered in the resistant NB cells, we treated FR-resistant KP-N-TK (FR-R) cells, KP-N-SIFA cells and FR-sensitive parental KP-N-TK cells with 10 μM FR and compared their intracellular ROS levels. Less FR-induced intracellular ROS were generated in the 2 resistant cell lines than in the sensitive KP-N-TK cells (Fig. 3*a*).

FR induced little phosphorylation of the kinases in the resistant KP-N-TK (FR-R) and KP-N-SIFA cells (Fig. 3*b*). Although phosphorylated JNK was present in KP-N-SIFA cells even in the absence of FR, FR did not increase its level during 48 hr.

DISCUSSION

FR is known to induce apoptosis in NB cells but the mechanism is not clear. Our results demonstrate that FR induced sustained-activation of JNK and p38 MAPK signaling in an ROS-dependent manner, and finally induced apoptosis in NB cells. In FR-resistant NB cells, FR failed not only to generate intracellular ROS but also to activate JNK and p38 MAPK signaling. Thus, the alterations in FR-resistant NB cells prevent FR from inducing apoptosis.

ROS are known to induce apoptosis. In KP-N-TK cells, FR induces prolonged production of intracellular ROS. FR-induced ROS generation precedes the processing of caspase-9, caspase-3 and PARP, indicating that ROS generation is upstream of the

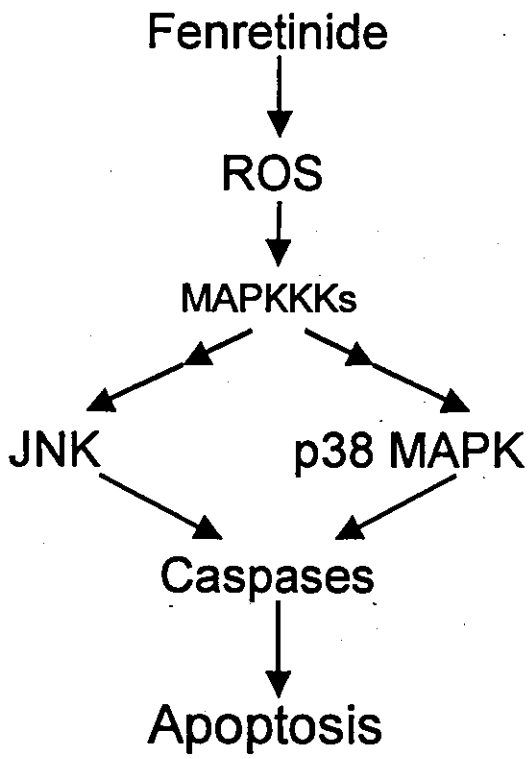

FIGURE 4 – Schematic representation of FR-induced ROS generation, JNK and p38 MAPK signaling and apoptosis in neuroblastoma cells. FR induces sustained-activation of JNK and p38 MAPK signaling in an ROS-dependent manner. The sustained activation of JNK and p38 MAPK activation leads to processing of caspases and apoptosis.

caspase cascade. The antioxidant AA almost completely blocked apoptosis and suppressed FR-induced intracellular ROS accumulation. Our results show that AA has a more complete inhibitory effect on FR-induced apoptosis in NB cells than on FR-induced apoptosis in other NB cell lines (CHLA-90, SMS-LHN, SMS-KCNR[7] and SH-SY5Y[8]).

FR activated both JNK and p38 MAPK in FR-sensitive KP-N-TK NB cells. In KP-N-TK cells, the activation of JNK and p38 MAPK by FR (starting after 4 hr of FR treatment) preceded the cleavages of caspase-9, caspase-3 and PARP (starting after 24 hr of FR treatment), indicating that the JNK and p38 MAPK signaling pathways are upstream of the caspase cascades, as reported in the LNCap and PC3 prostate carcinoma cell lines.[16,17] Furthermore, FR-induced activation of JNK and p38 MAPK is sustained for 48 hr, suggesting the possible role of the signaling in FR-induced apoptosis.[13–15] Interestingly, in prostate carcinoma LNCap cells, FR activated JNK but not p38 MAPK.[16]

Our finding that FR-induced activation of JNK and p38 MAPK in NB cells was ROS-dependent is supported by the finding that AA suppressed FR-induced activation of JNK and p38 MAPK signaling in KP-N-TK cells. In prostate carcinoma cells, Chen *et al.*[16] found that FR-induced JNK activation was not affected by the antioxidant *N*-acetyl-L-cysteine (NAC), indicating that FR activated JNK independent of ROS. They did not, however, determine whether NAC suppressed the accumulation of FR-induced intracellular ROS. In our present study, AA clearly reduced FR-induced intracellular ROS accumulation.

JNK and p38 MAPK pathways have been shown to be involved in ROS-induced apoptosis.[13,14] When ROS production is low, JNK and p38 MAPK are only transiently activated, and cells will survive.[13,14] On the contrary, high ROS production induces sustained-activation of JNK and p38 MAPK, and finally leads to cell death.[13,14] The quantity and duration of oxidative stress will determine which MAPK kinase kinases (MAPKKK) are activated, which will determine the activation pattern of JNK and p38 MAPK, which, in turn, will decide cell fate.[13,14]

ROS activate various signaling pathways other than MAPKKK, including c-Abl tyrosine kinase.[14] c-Abl activates both JNK and p38 MAPK in the response to DNA damage[22] and also mediates ROS-induced apoptosis under some conditions.[23] The c-Abl-p38 MAPK-p73 pathway is thought to be essential for apoptosis induced by chemotherapeutic agents.[24] This pathway might be also involved in fenretinide-induced apoptosis, although we did not examine the expression of p73 in these cells.

FR failed to induce intracellular ROS accumulation in the FR-resistant KP-N-TK (FR-R) and KP-N-SIFA NB cell lines, indicating that suppression of the ROS-productive system is responsible for the resistance to FR in NB cells. Similarly, FR produced less free radicals in FR-resistant SH-SY5Y cells.[8] ROS production in the FR-resistant A2780 ovarian cancer cell line was not significantly different from that in the FR-sensitive parental cells.[21] In FR-resistant NB cells, FR failed to activate JNK and p38 MAPK signaling. This result further supports the hypothesis that FR activates JNK and p38 MAPK signaling in an ROS-dependent manner. It also indicates that sustained-activation of JNK and p38 MAPK is responsible for FR-induced apoptosis. It is of interest to know whether these FR-resistant cells are also resistant to other cytotoxic agents, especially ROS-producing ones such as cisplatin. In our preliminary results, FR-resistant KP-N-SIFA cells were the most sensitive to cisplatin among the cell lines used in our study (data not shown). KP-N-TK cells, as well as KP-N-TK (FR-R) cells, were resistant to 20 μM cisplatin (data not shown). These data suggest that the mechanisms of FR resistance and cisplatin resistance are different.

In conclusion, we demonstrated for the first time that FR induces sustained activation of JNK and p38 MAPK in an ROS-dependent manner in FR-sensitive NB cells (Fig. 4), but not in FR-resistant cells. Moreover, our results raise the possibility that sustained-activation of the stress signaling pathway mediates FR-induced apoptosis. Our results also show for the first time that suppression of the intracellular ROS productive system and the downstream JNK/p38 MAPK pathways are related to FR-resistance in NB cells.

ACKNOWLEDGEMENTS

We gratefully acknowledge Dr. H. Ichijo (Laboratory of Cell Signaling, Graduate School of Pharmaceutical Sciences, The University of Tokyo) and all the members of our laboratory for their valuable discussions and support.

REFERENCES

1. Matthay KK, Castleberry RP. Treatment of advanced neuroblastoma. The US experience. In: Brodeur GM, Sawada T, Tsuchida Y, Voute PA, eds. Neuroblastoma. Amsterdam: Elsevier Science Publishers B.V., 2000. 417–36.
2. Sugimoto T, Sawada T, Matsumura T, Horii Y, Kemshead JT, Suzuki Y, Okada M, Tagaya O, Hino T. Morphological differentiation of human neuroblastoma cell lines by a new synthetic polyprenoic acid (E5166). Cancer Res 1987;47:5433–8.
3. Matthay KK, Villablanca JG, Seeger RC, Stram DO, Harris RE, Ramsay NK, Swift P, Shimada H, Black CT, Brodeur GM, Gerbing RB, Reynolds CP. Treatment of high-risk neuroblastoma with intensive chemotherapy, radiotherapy, autologous bone marrow transplantation, and 13-cis retinoic acid. N Engl J Med 1999;341:1165–73.
4. Wu JM, DiPietrantonio AM, Hsieh T-C. Mechanism of fenretinide (4-HPR)-induced cell death. Apoptosis 2001;6:377–88.
5. Rotmensz N, De Palo G, Formelli F, Costa A, Marubini E, Campa T, Crippa A, Danesini GM, Delle Grottaglie M, Di Mauro MG, Filiberti A, Gallazzi M, et al. Long-term tolerability of fenretinide (4-HPR) in breast cancer patients. Eur J Cancer 1991;27:1127–31.
6. Garaventa A, Luksch R, Lo Piccolo MS, Cavadini E, Montaldo PG,

Pizzitola MR, Boni L, Ponzoni M, Decensi A, De Bernardi B, Bellani FF, Formelli F. Phase I trial and pharmacokinetics of fenretinide in children with neuroblastoma. Clin Cancer Res 2003;9:2032–9.
7. Maurer BJ, Metelitsa LS, Seeger RC, Cabot MC, Reynolds CP. Increase of ceramide and induction of mixed apoptosis/necrosis by N-(4-hydroxyphenyl)-retinamide in neuroblastoma cell lines. J Natl Cancer Inst 1999;91:1138–46.
8. Lovat PE, Ranalli M, Annichiarrico-Petruzzelli M, Bernassola F, Piacentini M, Malcolm AJ, Pearson ADJ, Melino G, Redfern CPF. Effector mechanisms of fenretinide-induced apoptosis in neuroblastoma. Exp Cell Res 2000;260:50–60.
9. Lovat PE, Oliverio S, Ranalli M, Corazzari M, Rodolfo C, Bernassola F, Aughton K, Maccarrone M, Campbell Hewson QD, Pearson ADJ, Melino G, Piacentini M, et al. GADD153 and 12-lipoxygenase mediate fenretinide-induced apoptosis of neuroblastoma. Cancer Res 2002;62:5158–67.
10. Maurer BJ, Melton L, Billups C, Cabot MC, Reynolds CP. Synergistic cytotoxicity in solid tumor cell lines between N-(4-hydroxyphenyl)-retinamide and modulators of ceramide metabolism. J Natl Cancer Inst 2000;92:1897–909.
11. Wang H, Maurer BJ, Reynolds CP, Cabot MC. N-(4-hydroxyphenyl)-retinamide elevates ceramide in neuroblastoma cell lines by coordinate activation of serine palmitoyltransferase and ceramide synthase. Cancer Res 2001;61:5102–5.
12. Kyriakis JM, Avruch J. Mammalian mitogen-activated protein kinase signal transduction pathways activated by stress and inflammation. Physiol Rev 2001;81:807–69.
13. Matsuzawa A, Nishitoh H, Tobiume K, Takeda K, Ichijo H. Physiological roles of ASK1-mediated signal transduction in oxidative stress- and endoplasmic reticulum stress-induced apoptosis: advanced findings from ASK1 knockout mice. Antioxid Redox Signal 2002;4:415–25.
14. Martindale JL, Holbrook NJ. Cellular response to oxidative stress: signaling for suicide and survival. J Cell Physiol 2002;192:1–15.
15. Xia Z, Dickens M, Raingeaud J, Davis RJ, Greenberg ME. Opposing effects of ERK and JNK-p38 MAP kinases on apoptosis. Science 1995;270:1326–31.
16. Chen Y-R, Zhou G, Tan T-H. c-Jun N-terminal kinase mediates apoptotic signaling induced by N-(4-hydroxyphenyl)retinamide. Mol Pharmacol 1999;56:1271–9.
17. Shimada K, Nakamura M, Ishida E, Kishi M, Yonehara S, Konishi N. Contributions of mitogen-activated protein kinase and nuclear factor kappa B to N-(4-hydroxyphenyl)- retinamide-induced apoptosis in prostate cancer cells. Mol Carcinogen 2002;35:127–37.
18. Ulukaya E, Pirianov G, Kurt MA, Wood EJ, Mehmet H. Fenretinide induces cytochrome c release, caspase 9 activation and apoptosis in the absence of mitochondrial membrane depolarization. Cell Death Differ 2003;10:856–9.
19. Kuroda H, Sugimoto T, Horii Y, Sawada T. Signaling pathway of ciliary neurotrophic factor in neuroblastoma cell lines. Med Pediatr Oncol 2001;36:118–21.
20. Sugimoto T, Horii Y, Hino T, Kemshead JT, Kuroda H, Sawada T, Morioka H, Imanishi J, Inoko H. Differential susceptibility of HLA class II antigens induced by γ-interferon in human neuroblastoma cell lines. Cancer Res 1989;49:1824–8.
21. Appierto V, Cavadini E, Pergolizzi R, Cleris L, Lotan R, Canevari S, Formelli F. Decrease in drug accumulation and in tumour aggressiveness marker expression in a fenretinide-induced resistant ovarian tumour cell line. Br J Cancer 2001;84:1528–34.
22. Kharbanda S, Yuan Z-M, Weichselbaum R, Kufe D. Determination of cell fate by c-Abl activation in the response to DNA damage. Oncogene 1998;17:3309–18.
23. Sun X, Majumder P, Shioya H, Wu F, Kumar S, Weichselbaum R, Kharbanda S, Kufe D. Activation of the cytoplasmic c-Abl tyrosine kinase by reactive oxygen species. J Biol Chem 2000;275:17237–40.
24. Melino G, De Laurenzi V, Vousden KH. p73: Friend or foe in tumorigenesis. Nat Rev Cancer 2002;2:605–15.

Leukemia & Lymphoma, April 2004 Vol. 45 (4), pp. 825–828

Taylor&Francis
healthsciences

Acute Renal Failure Due to Leukemic Cell Infiltration Followed by Relapse at Multiple Extramedullary Sites in a Child with Acute Lymphoblastic Leukemia

ATSUSHI SATO[a], MASUE IMAIZUMI[a,b,*], SHUJI CHIKAOKA[a], HIDETAKA NIIZUMA[a], YOSHIYUKI HOSHI[a], JUNJI TAKEYAMA[c], KUNIHIRO FUJII[a], TOSHIYUKI NISHIO[a], MIKA WATANABE[c], CHIHAYA MAESAWA[d], YUTAKA HAYASHI[b] and KAZUIE IINUMA[a]

[a]Department of Pediatrics, Tohoku University School of Medicine, Sendai, Japan; [b]Department of Pediatric Hematology and Oncology, Tohoku University School of Medicine, Sendai, Japan; [c]Department of Pathology, Tohoku University School of Medicine, Sendai, Japan; [d]Department of Pathology, Iwate Medical University School of Medicine, Morioka, Japan

(Received 2 June 2003)

Acute renal failure due to leukemic infiltration into the kidney is rare in childhood acute lymphoblastic leukemia (ALL). We report here a five year-old boy with ALL who presented acute renal failure caused by leukemic infiltration at onset. Treatment with predonisolone and hemodialysis was effective. However, he showed persistent or repeated relapses at extramedullary sites, such as central nervous system, testis, and pancreas, suggesting that leukemic cells of this patient may have had a high affinity to extramedullary organs. On the basis of previous reports and the experience of this patient, intensive treatment may be needed in ALL children with renal involvement.

Keywords: ALL; Child; Acute renal failure; Extramedullary relapse

INTRODUCTION

It has been previously reported that renal infiltration causing kidney enlargement was found in 4–47% of children with acute lymphoblastic leukemia (ALL) by renal scintigraphy, intravenous pyelography or ultrasonography [1–6]. However, most of these children showed no acute renal failure and it developed in only 1% of children with ALL [7]. To our knowledge, there have been few reports of childhood ALL in which acute renal failure was caused by renal infiltration. We report here a boy with ALL who presented acute renal failure due to the leukemic infiltration at onset. Interestingly, this patient exhibited persistent or repeated extramedullary relapses at central nervous system (CNS), testis and pancreas, even after having achieved complete remission (CR) at bone marrow. In this patient, it was noted that leukemic cells could be predisposed to have a high affinity to extramedullary sites.

A CASE REPORT

A five year-old boy, who had presented with face edema and oliguria a few days earlier, was transferred to our hospital in September 2001. In our hospital, physical examination revealed hypertension (136/100 mmHg), hepatomegaly. No lymphadenopathy was observed and both kidneys were not palpable. Examination with abdominal computed tomography (CT) and ultrasonography revealed an enlargement of the bilateral kidneys (Fig. 1). Biochemical examination revealed lactate dehydrogenase of 2164 IU/L, blood urea nitrogen (BUN) of 23 mg/dl, creatinine (Cr) of 2.3 mg/dl, uric acid (UA) of 5.4 mg/dl. Urinalysis showed a specific gravity of 1.015 and proteinuria without hematuria or pyuria. White blood cell count (WBC) of the peripheral blood was 3.2×10^9/l with no appearance of blasts, hemoglobin was 10.3 g/dl, and platelet counts 195×10^9/l. Although bone marrow of the patient was dry tap in our hospital, bone marrow examination in the previous hospital showed 30% of lymphoblasts with L1 morphology of FAB

*Corresponding author. Address: Department of Pediatric Hematology and Oncology, Tohoku University School of Medicine, 1-1 Seiryo-machi, Aoba-ku, Sendai 980-8574, Japan. Tel.: 81-22-717-7287. Fax: 81-22-717-7290. E-mail: mimaizumi@ped.med.tohoku.ac.jp

ISSN 1042-8194 print/ISSN 1029-2403 online
DOI: 10.1080/10428190310001593148

classification and negative peroxidase and esterase stainings (Fig. 2A). The cytogenetic study of cells obtained from biopsy marrow materials showed normal karyotye. The histopathologic study of renal biopsy showed a massive and diffuse infiltration of mononuclear cells in the renal interstitium (Fig. 2B).

These cells were positive for CD79α, CD20, CD45, and negative for CD2, CD3, CD4, CD7, CD34, CD56, and myeloperoxidase (Fig. 2C). Furthermore, lumbar puncture showed 266/μl of lymphoblasts with surface markers positive for CD10, CD19, CD20, and CD22, and negative for CD3, and surface immunoglobulins. Immunological studies at the onset were performed only for the samples obtained from the kidney and CNS fluid. On the basis of these findings, he was diagnosed as ALL with renal and CNS infiltration.

He received hemodialysis immediately from the first day of admission, as well as administration of predonisolone. With these treatments, acute renal failure and dyspnea were rapidly relieved and hemodialysis was completed by the fourth day of admission. Evaluation with ultrasonography confirmed that the renal size of the patient decreased gradually to normal levels.

After the completion of hemodialysis, the patient was treated according to the medium-risk group arm of ALL-BFM 90 protocol [8] without delay in the schedule. However, CNS disease was persistent. With additional intrathecal therapy, CR was achieved after 4 months of treatment, but the right testicular and CNS relapse occurred during the subsequent treatment. After irradiation to both testes, he received bone marrow transplantation (BMT) from his HLA-mismatched mother in the state with CNS relapse in March 2002, followed by intrathecal therapy after BMT. However, 4 months after BMT, the second testicular relapse occurred. With his left relapsed testis removed and right testis irradiated, he achieved CR. In December 2002, he had abdominal pain with increased serum amylase levels, and abdominal CT demonstrated an enlargement of the pancreas (Fig. 3). Pancreatic relapse was confirmed by histological examination of the biopsy material showing pancreatic infiltration of lymphoblasts. He received intensive chemotherapy as of January 2003. In addition, we evaluated the state of minimal residual disease (MRD) of his bone marrow after he received BMT by detecting leukemic cell-specific IgH rearrangement using allele-specific oligonucleotide real-time polymerase chain reaction as previously reported [9]. This MRD examination revealed that his bone marrow retained CR at the molecular level, despite the frequent and multiple relapses at extramedullary sites (Data not shown).

FIGURE 1 Abdominal CT scan demonstrating a diffuse enlargement of the bilateral kidneys.

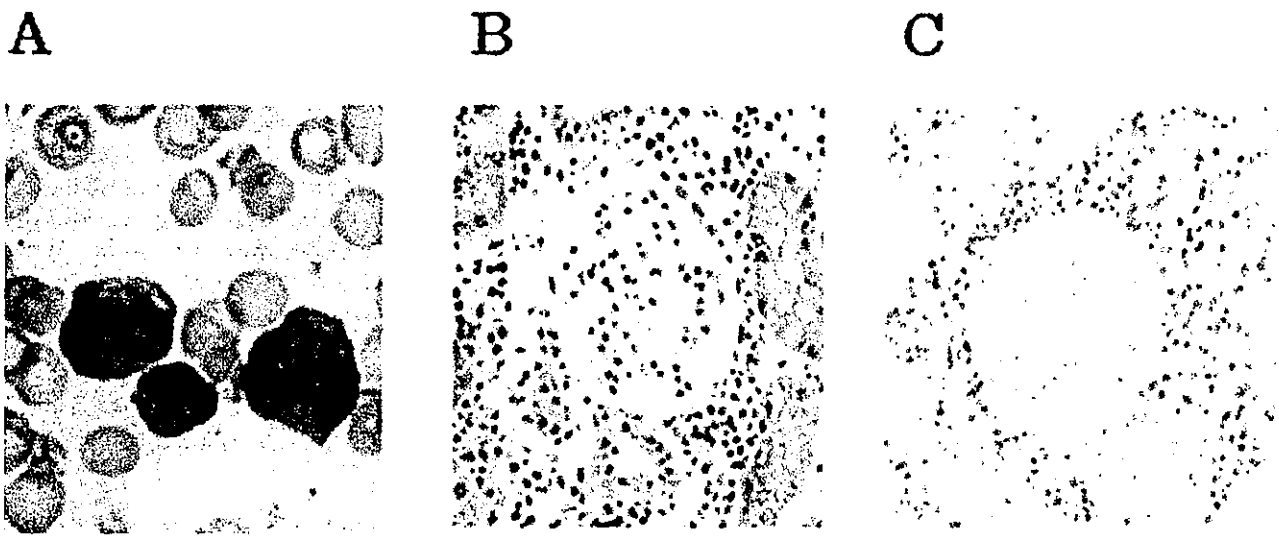

FIGURE 2 (A) Lymphoblasts in bone marrow at onset (May–Giemsa stain; magnification × 1000). (B) Renal biopsy specimen that lymphoblasts with irregular nuclear outline and fine chromatin showed massive and diffuse infiltration into the interstitium and glomeruli of the kidneys (Hematoxylin-eosin stain; magnification × 400). (C) The immunohistological stain of renal biopsy specimen for CD79α, a marker of B-cell lineage. Lymphoblasts positive for CD79α infiltrated into the interstitium of the kidneys (magnification × 400).

FIGURE 3 Abdominal CT scan demonstrating an enlargement of the pancreas head.

DISCUSSION

Acute renal failure was rarely seen in children who had renal enlargement at onset and there have been few reports in which acute renal failure was caused by the leukemic cell infiltration into the kidneys in childhood ALL. To our knowledge, 7 patients have been reported as individual case reports [6, 10–15]. All of the patients showed enlargement of the bilateral kidneys and elevation of the serum Cr levels. In 3 out of 7 patients [11, 13, 14], renal infiltration of leukemic cells was confirmed histologically. Tumor lysis syndrome was unlikely to be the cause of acute renal failure in our patient, because he showed no apparent elevation of serum UA and BUN in contrast to the elevation of serum Cr. These uncommon findings of renal dysfunction may result from the fact that the interstitial infiltration of leukemic cells caused vascular stasis but did not directly damage the nephrons as described [15]. Therefore, for children with ALL who show acute renal failure, leukemic infiltration into the kidneys should be considered as one of possible causes and examination with ultrasonography may be useful for differential diagnosis and evaluation of therapeutic efficacy.

Out of the 7 patients reported above, 4 were treated with chemotherapy and 2 with radiotherapy. Furthermore, dialysis was performed simultaneously in 5 out of 6 children, leading to improvement from acute renal failure in all of the 5 children. Our patient had a good response to initial treatment of predonisolone combined with hemodialysis, suggesting that this combined treatment may be useful not only to remove the direct cause of renal failure, but also to lighten a renal burden caused by tumor lysis.

ALL blasts of our patient seemed to have a high affinity to multiple extramedullary organs, including pancreas as well as kidneys, CNS, and testes. Pancreatic infiltration of leukemic cells is very rare and only two reports demonstrated such cases of children [16, 17]. In literature, it is yet undetermined whether ALL blasts with renal infiltration have predisposition to invade into other extramedullary sites. However, several investigators have reported CNS involvement that occurs simultaneously with renal infiltration [10, 18]. Therefore, the caution against leukemic involvement into extramedullary organs may be needed for ALL patients who show renal infiltration. Chemokine receptor CXCR4 and its ligand stromal cell-derived factor-1 (SDF-1) may play important roles in the extravasation and trafficking of normal lymphocytes [19]. Recently, Crazzolara *et al.* showed that high levels of CXCR4 expression on the blasts of childhood ALL was associated with their clinical features of extramedullary infiltration [20]. Interaction between CXCR4 and SDF-1 may be involved in the mechanisms of ALL blasts with a high affinity to extramedullary sites.

Finally, prognostic significance of leukemic renal infiltration is yet controversial for children with ALL. Renal involvement may be associated with shorter survival in four reports [2, 4, 6, 21], whereas two reports demonstrated no prognostic significance for the outcome when analyzed after adjustment for the known prognostic factors [1, 5]. Our patient had the well-known poor prognostic factors such as CNS involvement at onset, non-CR status at day 33 of remission-induction treatment [8], and the early relapse [22]. However, it was noted that all of these prognostic factors in our patient were strongly linked with the leukemic cell property of the high affinity to invade into extramedullary organs. Therefore, this study suggests that extensive renal infiltration may be associated with a poor prognostic factor in childhood ALL that needs intensive treatment, although further investigation is needed.

Acknowledgements

Supported by grants from the Ministry of Education, Science and Culture, and the Ministry of Health and Public Welfare, Japan.

References

[1] Hann, I.M., Lees, P.D., Palmer, M.K., Gupta, S. and Morris-Jones, P.H. (1981) "Renal size as a prognostic factor in childhood acute lymphoblastic leukemia", *Cancer*, **48**, 207–209.

[2] Taccone, A., De Bernardi, B., Comelli, A., Dini, G., Bartolini, M., Banderali, A., Glorialanza, P. and Guglielmetto, E. (1982) "Renal changes in acute leukemia in children at onset. Incidence and prognostic value", *Pediatria Medica e Chirurgica*, **4**, 107–113.

[3] Kuntz, D.J., Leonard, J.C., Nitschke, R.M., Vanhoutte, J.J., Wilson, D.A. and Basmadjian, G.P. (1984) "An evaluation of diagnostic techniques utilized in the initial workup of pediatric patients with acute lymphocytic leukemia", *Clinical Nuclear Medicine*, **9**, 405–408.

[4] Rajantie, J., Jaaskelainen, J., Perkkio, M. and Siimes, M.A. (1986) "Kidneys very large at diagnosis are associated with poor prognosis in children with acute lymphoblastic leukemia", *American Journal of Pediatric Hematology and Oncology*, **8**, 87–90.

[5] Neglia, J.P., Day, D.L., Swanson, T.V., Ramsay, N.K., Robison, L.L. and Nesbit, M.E., Jr. (1988) "Kidney size at diagnosis of childhood acute lymphocytic leukemia: lack of prognostic significance for outcome", *American Journal of Pediatriac Hematology and Oncology*, **10**, 296–300.

[6] D'Angelo, P., Mura, R., Rizzari, C., Conter, V., Bellini, F., Valsecchi, M.G., Manganini, C., Silvestri, D. and Masera, G. (1995) "Prognostic value of nephromegaly at diagnosis of childhood acute lymphoblastic leukemia", *Acta Haematologica*, **94**, 84–89.

[7] Lundberg, W.B., Cadman, E.D., Finch, S.C. and Capizzi, R.L. (1977) "Renal failure secondary to leukemic infiltration of the kidneys", *American Journal of Medicine*, **62**, 636–642.

[8] Schrappe, M., Reiter, A., Ludwig, W.D., *et al.* (2000) "Improved outcome in childhood acute lymphoblastic leukemia despite reduced use of anthracyclines and cranial radiotherapy: results of trial ALL-BFM 90. German-Austrian-Swiss ALL-BFM Study Group", *Blood*, **95**, 3310–3322.

[9] Tarusawa, M., Yashima, A., Endo, M. and Maesawa, C. (2002) "Quantitative assessment of minimal residual disease in childhood lymphoid malignancies using an allele-specific oligonucleotide real-time quantitative polymerase chain reaction", *International Journal of Hematology*, **75**, 166–173.

[10] Stoffel, T.J., Nesbit, M.E., Levitt, S.H. (1975) "The role of radiotherapy in renal involvement in acute childhood leukemia", *Radiology*, **117**, 687–694.

[11] Gilboa, N., Lum, G.M., Urizar, R.E. (1983) "Early renal involvement in acute lymphoblastic leukemia and nonHodgkin's lymphoma in children", *Journal of Urology*, **129**, 364–367.

[12] Moudgil, A., Ray, D., Vasudev, A.S. and Srivastava, R.N. (1989) "Acute renal failure due to renal infiltration with lymphoreticular malignant cells", *Indian Pediatrics*, **26**, 830–832.

[13] Gupta, A., Malhotra, H.S., Kumar, L., Sirwal, I.A., Sakhuja, V. and Chugh, K.S. (1990) "Acute renal failure due to leukaemic infiltration of kidneys", *Journal of the Association of Physicians of India*, **38**, 284–286.

[14] Bunchman, T.E., Gale, G.B., O'Connor, D.M., Salinas-Madrigal, L. and Chu, J.Y. (1992) "Renal biopsy diagnosis of acute lymphocytic leukemia", *Clinical Nephrology*, **38**, 142–144.

[15] Dahlbeck, S.W., Tome, M., Kagan, A.R. and Cooper, R. (2001) "The role of radiation therapy in children with acute lymphoblastic leukemia kidney infiltration", *Medical and Pediatric Oncology*, **37**, 477–478.

[16] Biurrun Mancisidor, C., Vega Eraso, J., Agote Jemein, A., Echeberria Lizarraga, A., Ruiz Benito, C. and Nogues Perez, A. (1991) "Pancreatic infiltration in lymphoblastic leukemia. Ultrasonic findings", *Anales Españoles de Pediatria*, **34**, 170–172.

[17] Rausch, D.R., Norton, K.I., Glass, R.B. and Kogan, D. (2002) "Infantile leukemia presenting with cholestasis secondary to massive pancreatic infiltration", *Pediatric Radiology*, **32**, 360–361.

[18] Gupta, S., Keane, S. (1985) "Renal enlargement as a primary presentation of acute lymphoblastic leukaemia", *British Journal of Radiology*, **58**, 893–895.

[19] Nagasawa, T., Tachibana, K., Kishimoto, T. (1998) "A novel CXC chemokine PBSF/SDF-1 and its receptor CXCR4: their functions in development, hematopoiesis and HIV infection", *Seminars in Immunology*, **10**, 179–185.

[20] Crazzolara, R., Kreczy, A., Mann, G., Heitger, A., Eibl, G., Fink, F.M., Mohle, R. and Meister, B. (2001) "High expression of the chemokine receptor CXCR4 predicts extramedullary organ infiltration in childhood acute lymphoblastic leukaemia", *British Journal of Haematology*, **115**, 545–553.

[21] Taylor, G.A., Mellits, E.D., Zinkham, W.H. and Leventhal, B.G. (1982) "Prognostic role of the intravenous urogram in children with acute leukemia", *Medical and Pediatric Oncology*, **10**, 489–496.

[22] Feig, S.A., Harris, R.E. and Sather, H.N. (1997) "Bone marrow transplantation versus chemotherapy for maintenance of second remission of childhood acute lymphoblastic leukemia: a study of the Children's Cancer Group (CCG-1884)", *Medical and Pediatric Oncology*, **29**, 534–540.

Available online at www.sciencedirect.com
SCIENCE DIRECT®
Leukemia Research 28 (2004) 959–967
Leukemia Research
www.elsevier.com/locate/leukres

Alteration in the cellular response to retinoic acid of a human acute promyelocytic leukemia cell line, UF-1, carrying a patient-derived mutant PML-RARα chimeric gene

Atsushi Sato[a], Masue Imaizumi[a,b,*], Yoshiyuki Hoshi[a], Takeshi Rikiishi[a], Kunihiro Fujii[a], Masahiro Kizaki[c], Hiroyuki Kagechika[d], Akira Kakizuka[e], Yutaka Hayashi[b], Kazuie Iinuma[a]

[a] *Department of Pediatrics, Tohoku University School of Medicine, 1-1 Seiryo-machi, Aoba-ku, Sendai 980-8574, Japan*
[b] *Department of Pediatric Hematology and Oncology, Tohoku University School of Medicine, 1-1 Seiryo-machi, Aoba-ku, Sendai 980-8574, Japan*
[c] *Division of Hematology, Keio University School of Medicine, Tokyo, Japan*
[d] *Faculty of Pharmaceutical Sciences, Tokyo University, Tokyo, Japan*
[e] *Department of Functional Biology, Kyoto University Graduate School of Biostudies, Kyoto, Japan*

Received 20 August 2003; accepted 31 December 2003

Available online 17 April 2004

Abstract

Cellular response to all-*trans* retinoic acid (ATRA) of acute promyelocytic leukemia (APL) with patient-derived mutant PML-retinoic acid receptor-α (PML-RARα) was investigated using an APL cell line, UF-1, carrying Arg611Trp mutation in PML-RARα. Although the mutant protein showed a decreased ligand-dependent transcriptional activity and retained a dominant-negative effect on normal RARα, UF-1 cells underwent growth inhibition, maturation and apoptosis in response to ATRA at 1 μM, but not ≤100 nM, after 4 days of treatment with ATRA. Moreover, in the presence of 1 μM ATRA, approximately 50% of UF-1 cells expressing annexin V, an early-apoptotic marker, was negative for CD11b and showed immature morphology. These findings suggest that UF-1 cells, despite expressing mutant PML-RARα protein, can be induced by ATRA to undergo differentiation and apoptosis through RA-inducible mechanism(s), in which a proportion of apoptosis may occur independent of terminal differentiation. This unique cell line may be useful for investigating the pathogenesis of ATRA resistance and the mechanism of ATRA-induced apoptosis in APL.

Keywords: Acute promyelocytic leukemia; Retinoic acid; Apoptosis; Differentiation; Mutant PML-RARα

1. Introduction

Acute promyelocytic leukemia (APL) is characterized by a blockade of myeloid maturation at the promyelocyte stage and by a 15;17 chromosomal translocation generating the PML-retinoic acid receptor-α (PML-RARα) chimeric protein, which inhibits normal RARα transcriptional activity in a dominant-negative fashion [1]. Differentiation of APL cells is induced by treatment all-*trans* retinoic acid (ATRA) at pharmacological doses, and, under such conditions, PML-RARα can respond to ATRA and show a ligand-dependent transcriptional activity as well as a decreased dominant-negative effect on normal RARα [2]. Although ATRA therapy is highly effective in inducing complete remission of patients with APL [3,4], some patients who become ATRA-resistant during relapse have a poor prognosis [3,5,6]. Recently, however, it has been shown that arsenic trioxide can induce complete remission in the majority of these relapsed patients [7,8].

ATRA resistance may be caused by increased oxidative catabolism of ATRA [9–11], or by mutations in the RARα portion of the chimeric PML-RARα gene [12–15]. Analysis of APL patients with ATRA resistance revealed three clusters of missense mutations in the PML-RARα chimeric gene. These mutations are located in the RARα portion of the chimeric protein that functions in ligand binding, receptor dimerization and ligand-dependent transcriptional activity [16]. In vitro transfection experiments revealed that the different mutations identified in patients with ATRA resistance had different effects on the RA-dependent transcription

Abbreviations: APL, acute promyelocytic leukemia; PML-RARα, PML-retinoic acid receptor-α; ATRA, all-*trans* retinoic acid; 9CRA, 9-*cis*-retinoic acid; RXR, retinoid X receptor

* Corresponding author. Tel.: +81-22-717-7287; fax: +81-22-717-7290.
E-mail address: mimaizumi@ped.med.tohoku.ac.jp (M. Imaizumi).

0145-2126/$ – see front matter © 2004 Elsevier Ltd. All rights reserved.
doi:10.1016/j.leukres.2003.12.017

process, suggesting that diverse molecular pathogeneses contribute to ATRA resistance due to mutant PML-RARα [15]. Experiments with primary cultures of APL cells from patients with ATRA resistance showed that ATRA sensitivity varied with different mutations in PML-RARα [14,17]. Although experimentally derived ATRA-resistant HL-60 or NB4 subclones have either complete loss of or a maturation defect in the response to RA [12,18–20], it is not known how APL cells derived from patients with ATRA resistance would respond to ATRA at the cellular level.

During ATRA therapy, APL cells are induced to enter the terminal stage of differentiation and are then cleared from the blood [21]. This process may be mediated by apoptosis because aged mature neutrophils are eliminated via apoptosis [22] and APL cells undergo apoptosis in response to ATRA therapy in vivo [21,23]. It has been suggested that restoration of PML function and normal RAR signaling may be involved in the mechanism(s) by which APL cells are stimulated to undergo apoptosis [20]. Thus, it is thought, but not yet proven, that ATRA induces apoptosis of APL cells independent of or prior to terminal differentiation.

Recently, Kizaki et al. [24] established an APL cell line, UF-1, from a patient who became ATRA resistant at relapse. This cell line expresses a short form of the PML-RARα protein with a missense mutation (Arg611Trp). This mutation impairs ATRA binding and reduces ATRA-sensitivity in vitro [25]. In the present study, we examined RA-induced differentiation and apoptosis of UF-1 cells and compared the cellular responses of UF-1 to RA with the molecular response of the mutant PML-RARα protein. Our findings suggest that regulation of RA signaling other than that through mutant PML-RARα may be involved in the cellular response of UF-1 to RA, and that ATRA may induce APL cells to undergo apoptosis not only as consequence of differentiation but also prior to terminal differentiation.

2. Materials and methods

2.1. Cell line

The UF-1 cell line was established and characterized by Kizaki et al. [24]. Cells were maintained in suspension culture in RPMI 1640 medium (Gibco-BRL, Grand Island, NY) with 10% fetal bovine serum (FBS) (Hyclone Laboratories Inc., Logan, UT) at 37 °C in a humidified atmosphere of 5% CO_2 in air. Cell numbers and viability were assessed with a hemocytometer and by trypan blue dye-exclusion test, respectively.

2.2. Retinoids

ATRA and 9-*cis*-retinoic acid (9CRA) were purchased from Sigma Chemical Co. (St. Louis, MO). HX600, a synthetic retinoid that acts as an retinoid X receptor (RXR)-specific agonist, was provided by Dr. H. Kagechika [26]. Stock solutions (1 mM) of retinoids in ethanol were diluted serially in ethanol and then added to cell cultures at the final concentrations indicated. The final concentration of ethanol in each culture was less than 0.1%.

2.3. Morphologic evaluation of apoptosis

Cell morphology was examined by light microscopy on cytospin slides stained with Wright-Giemsa. More than 200 cells for each sample were scored and evaluated for morphologic features of apoptosis, including nuclear condensation and fragmentation.

2.4. Nitroblue tetrazolium (NBT) reduction assay

The ability of cells to reduce NBT was assessed as previously described [27]. Briefly, 10^6 viable cells were suspended in 1 ml phosphate-buffered saline (PBS) containing 0.5 mg/ml NBT (Sigma) and 162 nM 12-O-tetradecanoylphorbol-13-acetate (TPA) (Sigma). After incubation at 37 °C for 25 min, the percentage of formosan-positive cells was determined on cytospin slides by Wright-Giemsa staining. With exclusion of dead cells, at least 200 intact cells per specimen were scored under light microscopy.

2.5. Flow cytometric analysis of CD11b expression

To evaluate cell differentiation, we analyzed expression of CD11b. Cells were washed twice with PBS and incubated with fluorescein isothiocyanate (FITC)-conjugated anti-CD11b monoclonal antibody (Coulter, Hialeah, FL) or with FITC-conjugated non-immune antibody as a negative control at 4 °C for 15 min. Cells were washed with PBS and analyzed on a FACScan (Becton Dickinson, Mountain View, CA) with Cell Quest software (Becton Dickinson).

2.6. Flow cytometric analysis of early apoptotic cells

To detect cells in the early phase of apoptosis, we analyzed expression of annexin V by flow cytometry. This method requires no permeabilization of the cell membrane and, therefore, is suitable for investigating the kinetics of differentiation and apoptosis at the single-cell level. After incubation with phycoerythrin (PE)-conjugated anti-CD11b antibody (Coulter) at 4 °C for 15 min, cells were washed with PBS and stained with FITC-conjugated annexin V and propidium iodide (PI) according to the manufacturer's instructions (Genzyme, Cambridge, MA). Flow cytometric analysis was performed with a FACScan, or three-color sorting was performed with an Epics Elite (Coulter). After gating PI (−) viable cells, annexin V (+) and CD11b (−) cells were analyzed and sorted for morphological evaluation. Annexin V (+) and PI (−) cells were considered to be in the early stage of apoptosis [28].

2.7. DNA extraction and agarose gel electrophoresis

DNA was extracted as previously reported but with slight modification [29]. Briefly, cell pellets were suspended in 1 ml TEN solution (10 mM Tris–Cl (pH 7.4), 25 mM EDTA, 100 mM NaCl). After addition of 100 μl 10% sodium dodecyl sulfate (SDS), 30 μg RNase A (Sigma), and 1 mg proteinase K (Sigma), the reactions were incubated overnight at 55 °C. DNA was extracted with phenol and precipitated with sodium acetate and isopropanol, and then DNAs (2 μg per sample) were separated by electrophoresis on 2% agarose gels, and stained with ethidium bromide.

2.8. Transfection assays of ligand-dependent transcriptional activity of PML-RARα chimeric protein

A full length of cDNA clone of PML-RARα with Arg611Trp mutation was derived from pCMX expression vector harboring a short form of the wild type PML-RARα cDNA using a site-directed mutagenesis kit (Stratagene, Cambridge, United Kingdom) [13]. The wild-type and mutant cDNA clones were used in transient transfection experiments for evaluating in vitro ligand-dependent transcriptional activity. COS-1 cells were seeded in six-well plates at 2×10^5 cells per well in 2 ml DMEM with 10% FBS 1 day prior to transfection. Transfection was performed with the Lipofectamine Plus kit (Gibco-BRL) as described previously [13]. Briefly, the transfection mixture (200 μl Opti-MEM I, 0.4 μg of pCMX expression vector encoding the short form of wild-type or mutant (Arg611Trp) PML-RARα, 0.4 μg of R140-Luciferase reporter plasmid, 0.2 μg of pCMV-β-galactosidase reporter plasmid, 6 μl PLUS reagent, and 6 μl Lipofectamine reagent) was overlaid onto cells and incubated for 6 h at 37 °C. The transfection mixture was then replaced with 2 ml DMEM containing 10% FBS and ATRA, 9CRA, or HX600 was added at various concentrations indicated. After 48 h of incubation, the cells were lyzed in 200 μl Report Lysis Buffer (Promega) and centrifuged at 15,000 rpm for 2 min, and then 20 μl of supernatant of the cell lysate was mixed with 100 μl luciferase assay reagent (Promega), and luciferase activity was measured with a luminometer (Atto Co., Tokyo, Japan). Values were normalized in reference to β-gal activity. For the analysis of the dominant-negative action of mutant PML-RARα, pCMX expression vectors encoding normal RARα mixed with that encoding wild-type or mutant-form PML-RARα chimeric gene, or pCMX vector alone (total 0.4 μg with a weight ratio of 1:3, respectively) were transfected into COS-1 cells with same protocol.

2.9. Statistical analysis

Student's *t*-test was used to determine statistical significance. Probability (*P*) values lower than 0.05 were considered significant.

3. Results

3.1. Time course of cell growth, viability, and NBT reduction of UF-1 cells induced by ATRA or 9CRA

Growth of UF-1 cells was slow (doubling time: 96 h), and proliferation was inhibited in the presence of 1 μM, but not ≤100 nM, ATRA after 4 days of culture (Fig. 1A), whereas growth inhibition was observed in the presence of 9CRA at 1 μM and 100 nM after 4 days of culture (Fig. 1B). Viability of UF-1 cells was markedly decreased after 6 days of culture in the presence of 1 μM ATRA or 9CRA (Fig. 1C and D). Viability of UF-1 remained above 90% in the presence of ATRA at doses below 100 nM, whereas cell viability decreased slightly in the presence of 100 nM 9CRA (Fig. 1C and D).

3.2. Morphology and NBT reduction of UF-1 in the presence of ATRA or 9CRA

Morphological analysis of UF-1 cells treated with 1 μM ATRA for 8 days revealed myeloid maturation and formation of apoptotic bodies, suggestive of differentiation with apoptosis (Fig. 2A). NBT Reduction by UF-1 cells was not observed at ≤100 nM, but it was increased at 1 μM ATRA, while NBT reduction was observed at 1 μM and 100 nM of 9CRA in a dose dependent manner (Fig. 1E and F). At 8 days of culture, the degree of NBT reduction induced by 10 nM or 100 nM 9CRA was low but significantly higher than that induced by 10 nM or 100 nM ATRA ($P < 0.01$) (Fig. 2B). Similar findings were observed for expression of CD11b (data not shown).

3.3. Apoptosis of UF-1 cells induced by ATRA and 9CRA

Morphological evaluation revealed that ATRA at 1 μM, but not ≤100 nM, induced apoptosis of UF-1 cells, whereas 9CRA at ≥100 nM induced apoptosis in a dose-dependent manner (Fig. 3). Examination of DNA ladder formation confirmed that apoptosis occurred in response to 1 μM ATRA and ≥100 nM 9CRA (Fig. 4).

3.4. Effect of HX600 on ATRA-sensitivity of UF-1 cells

To evaluate the involvement of RXR activation in altered ATRA sensitivity, UF-1 cells were cultured in the presence of 100 nM ATRA, 1 μM HX600, or both. NBT reduction and apoptosis were not observed in response to ATRA or HX600 alone. However, in the presence of both compounds, the percentages of cells showing NBT reduction and apoptosis increased to 14.1±2.6% and 8.3±2.8%, respectively, which are levels similar to those induced by 100 nM 9CRA (Fig. 5).

3.5. Ligand-dependent transcriptional activity

As described previously [25], UF-1 cells contain a mutation (Arg611Trp) in the RARα E-domain of the

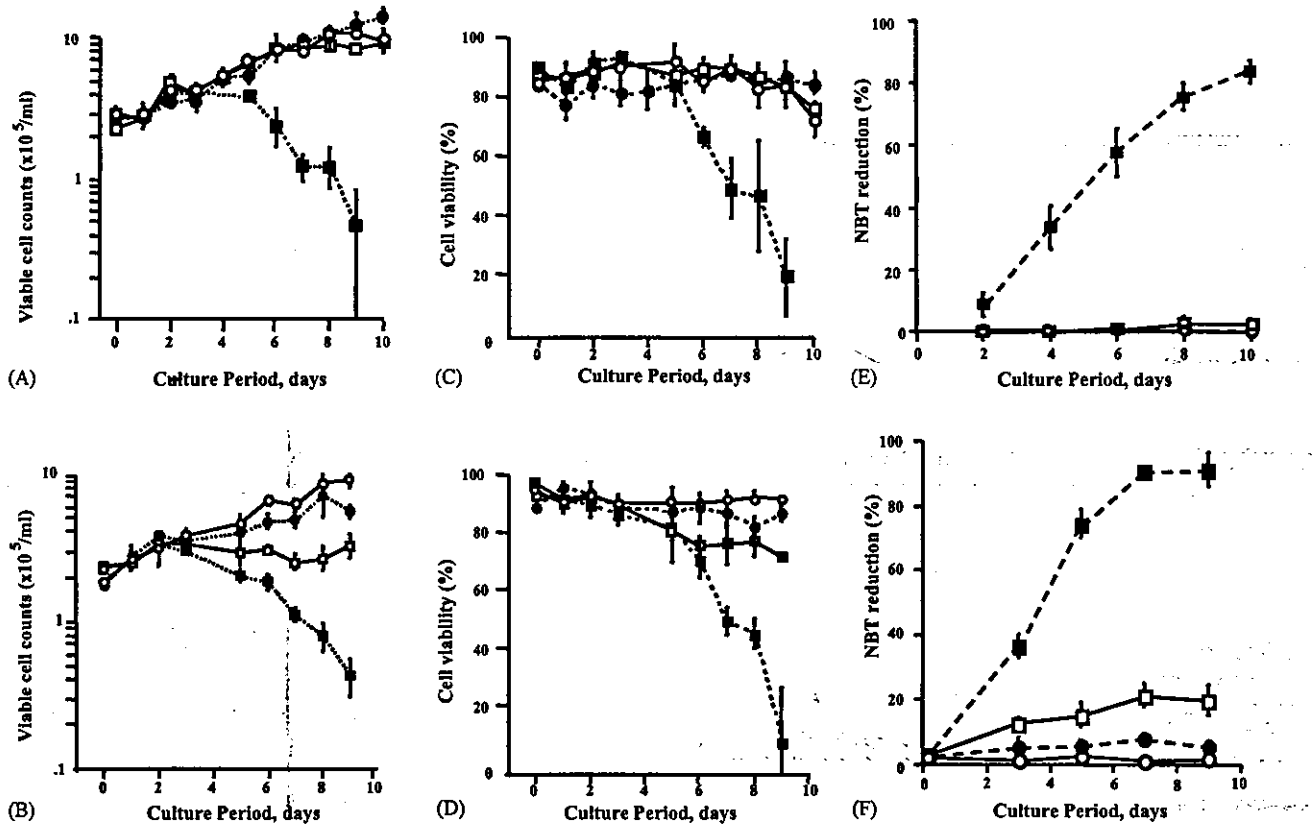

Fig. 1. Time course of viable cell number (A, B), cell viability (C, D) and NBT reduction (E, F) for UF-1 cells cultured in the absence (○) or presence of ATRA (A, C, E) or 9CRA (B, D, F). RA doses were: 10 nM (●), 100 nM (□), and 1 μM (■). NBT reduction analysis was performed with exclusion of dead cells on slides. Results are mean ± S.D. of three experiments.

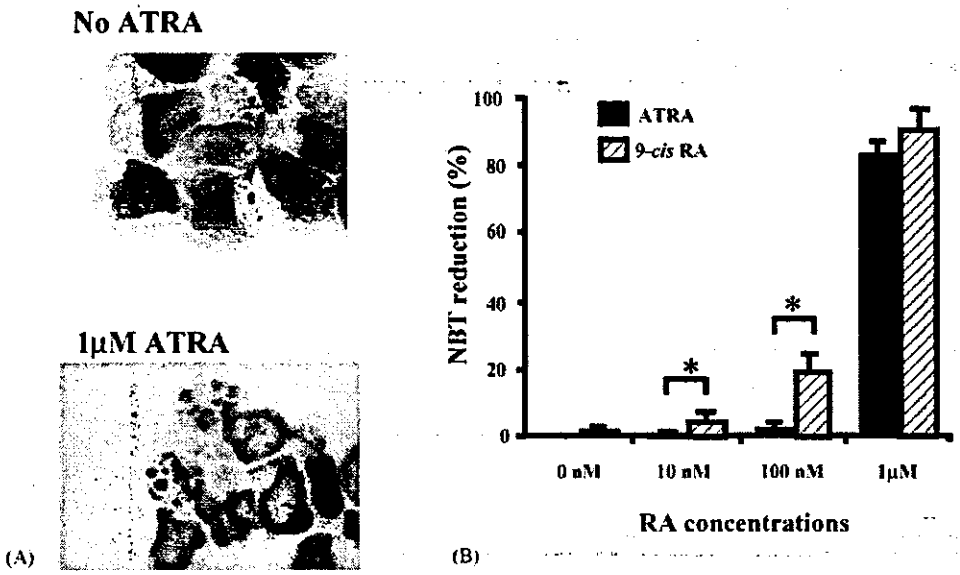

Fig. 2. (A) Morphological changes in UF-1 cells cultured for 8 days in the absence or presence of 1 μM ATRA. Wright-Giemsa staining of cells (1000× magnification). (B) NBT reduction in UF-1 cells treated with ATRA or 9CRA. After 8 days of culture in the presence of different concentrations of ATRA or 9CRA, UF-1 cells were tested for NBT reduction. Bars are *mean* ± S.D. of three experiments (* $P < 0.05$).